RSC Advances

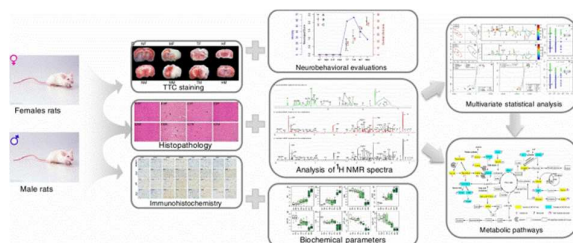# Gender-specific metabolic responses in focal cerebral ischemia of rats and Huang-Lian-Jie-Du decoction treatment

Journal:	*RSC Advances*
Manuscript ID	RA-ART-09-2015-019934.R1
Article Type:	Paper
Date Submitted by the Author:	27-Oct-2015
Complete List of Authors:	Zhang, Qian; China Pharmaceutical University, State Key Laboratory of Natural Medicines, Department of Natural Medicinal Chemistry Guo, Pingping; China Pharmaceutical University, State Key Laboratory of Natural Medicines, Department of Natural Medicinal Chemistry Wang, Junsong; Nanjing University of Science and Technology, School of Environmental and Biological Engineering Yang, Ming-Hua; China Pharmaceutical University, Department of Natural Medicinal Chemistry Kong, Ling-Yi; China Pharmaceutical University, Department of Natural Medicinal Chemistry
Subject area & keyword:	Systems biology < Biological

SCHOLARONE™
Manuscripts

Gender-specific metabolic responses in focal cerebral ischemia of rats and Huang-Lian-Jie-Du decoction treatment

Qian Zhang[a], Pingping Guo[a], Junsong Wang*[b], Minghua Yang[a], Lingyi Kong*[a]

Novelty of the work:

^{1}H NMR based metabolomics approach combined with neurobehavioral evaluations, cerebral infarct assessments, biochemical evaluations, histological inspections and immunohistochemistry observations was successfully applied to explore gender-specific metabolic differences in ischemic stroke and the protective effect of Huang-Lian-Jie-Du decoction (HLJDD).

1 **Gender-specific metabolic responses in focal cerebral ischemia of rats**

2 **and Huang-Lian-Jie-Du decoction treatment**

3

4 Qian Zhang[a], Pingping Guo[a], Junsong Wang*[b], Minghua Yang[a], Lingyi Kong*[a]

5

6 [a]*State Key Laboratory of Natural Medicines, Department of Natural Medicinal Chemistry, China*

7 *Pharmaceutical University, 24 Tong Jia Xiang, Nanjing 210009, PR China. Fax/Tel:*

8 *86-25-8327-1405; E-mail: cpu_lykong@126.com*

9 [b]*Center for Molecular Metabolism, Nanjing University of Science & Technology, 200 Xiao Ling Wei*

10 *Street, Nanjing 210094, PR China. Fax/Tel: 86-25-8431-5512; E-mail: wang.junsong@gmail.com*

11

12 *Corresponding author: Prof. Lingyi Kong and Prof. Junsong Wang

13

14

15

16

17

18

19

20

21

22

23

Abstract

24

25   This study aims to explore gender-specific metabolic differences in ischemic stroke

26   and the protective effect of HLJDD using NMR-based metabolomics techniques. A

27   unilateral middle cerebral artery occlusion (MCAO) rat model was established to

28   achieve cerebral ischemia. Rats were orally administrated with the extract of

29   Huang-Lian-Jie-Du decoction once a day for ten consecutive days to study its

30   therapeutic effect. ^{1}H NMR-based metabolomics approach combined with pattern

31   recognition approaches was applied to explore gender-specific metabolic profiling of

32   serum, cerebrum and cerebellum extracts. Oxidative stress, energy metabolism, fat and

33   amino acid metabolism were significantly perturbed in male MCAO rats, while only

34   oxidative stress and amino acid metabolism were perturbed in female MCAO rats.

35   These results complemented with neurobehavioral evaluations, cerebral infarct

36   assessments, biochemical evaluations, histological inspections and

37   immunohistochemistry observations strongly demonstrated that gender play an

38   important role in the process of neuronal damage triggered by cerebral

39   ischemia-reperfusion injury, and female rats are more resistant to ischemic stroke than

40   male rats. Furthermore, HLJDD was found to treat ischemic stroke in a gender

41   dependent manner and females gain a relatively greater benefit than males from

42   HLJDD therapy. This study built a substantial basis for further systematic study on the

43   underlying mechanisms involved in these gender differences in ischemic stroke. These

44   findings also highlight the need to take gender differences into account in the

45   treatment of stroke and the development of its therapy strategies.

1. Introduction

Cerebral stroke, one of the most common neurological disorders, is the third leading cause of mortality in industrialized countries (ranking behind heart diseases and various cancers), and the most frequent cause of permanent disability in adults worldwide.[1] It can be classified into two major categories: ischemic and hemorrhagic,[2] and the former comprised of almost 80% of strokes.[3] It is now well recognized that, the epidemiology of ischemic stroke is sexually dimorphic in that ischemic events occur with greater frequency and stroke induced brain damage is more severe in men than in women, regardless of country-of-origin and ethnic culture.[4, 5]

Gender differences are of interest from a variety of perspectives and have been the focus for many years. Females and males are also known to have different abilities to manage diseases.[6] In drug discovery and development, gender differences have been extensively studied in pharmacokinetics (absorption, distribution, metabolism, excretion) and pharmacodynamics (efficacy and toxicity).[7-9] In recent years, metabolic profiling has been used to identify gender differences in human or animals in a number of studies.[10-16]

Metabolomics provides a whole-organism biological description of multivariate metabolic responses to a perturbation via analytical techniques such as NMR, LC-MS, and GC-MS. As an unbiased, noninvasive, high-throughput and rapid analysis technique,[17, 18, 19] NMR has been one of the most widely utilized approaches in metabolomics analyses. What's more, NMR based metabolomics provides a detailed and specific insight into the integrated function of a complex bio-system at a system

68   level and cellular metabolic processes under normal and altered (i.e. disease-related)

69   conditions,[20, 21] thus simplifying the mechanistic study of complex traditional Chinese

70   medicine (TCM).[22]

71   Huang-Lian-Jie-Du Decoction (HLJDD), a representative TCM formula, has long

72   been used to treat cerebral ischemia-reperfusion (CI/R) injury[23-25] and to promote the

73   regeneration of peripheral neuro.[26-28] However, these studies were made only in male

74   animals. We determined if there is a gender differences in cerebral ischemic outcome

75   after HLJDD preconditioning, and if this sex-specific response is linked to differences

76   in metabolic profiles.

77   In this study, a middle cerebral artery occlusion (MCAO) rat model was established

78   to imitate human ischemic stroke. Both male and female rats were used to understand

79   gender differences of cerebral ischemia and MCAO rats were treated with HLJDD to

80   explore its effects on male and female rats. A ^{1}H NMR-based metabolomics approach

81   was adopted to profile metabolites in serum, cerebrum and cerebellum samples

82   collected from both the females and males, complemented with the biochemical

83   evaluation, histological inspection and immunohistochemistry observations.

84

85   **2 Materials and methods**

86   2.1 Materials and the preparation of HLJDD

87   Sodium 3-trimethylsilyl-propionic acid (TSP) was purchased from Sigma (St. Louis,

88   MO, USA). Deuterium oxide (D_2O, 99.9 %) was bought from Sea Sky Bio

89   Technology Co. Ltd (Beijing, China). Chloral hydrate was obtained from Sinopharm

90   Chemical Reagent Co. Ltd (Shanghai, China). Ultra-pure distilled water, prepared

91   using a Milli-Q purification system, was utilized in the experiments.

92   HLJDD, composed of *Rhizoma coptidis* (*Coptis chinensis* Franch, Ranunculacea),

93   *Radix scutellariae* (*Scutellaria baicalensis* Georgi, Labiatae), *Cortex phellodendri*

94   (*Phellodendron chinensis* Schneid, Rutaceae) and *Fructus Gardeniae* (*Gardenia*

95   *jasminoides* Ellis, Rubiaceae), with the ratio of 3:2:2:3 (w/w/w/w), reaching a total

96   weight of 1.0 kg, was extracted with 70 % ethanol (1:10, w/v) under reflux for three

97   times, 1h each.[29-32] The extract solution were combined and freeze-drying in vacuum

98   to afford an extract of HLJDD (264.8 g, yield: 26.48 %), which was dissolved in 0.5 %

99   CMC-Na (carboxymethyl cellulose sodium salt) to the final concentration of 5.0 g/ml

100 (equivalent to dry weight of raw materials) before intragastrical (ig.) administration.

101 All herbs were purchased from Jiangsu Medicine Company (Nanjing, China), and

102 authenticated by Professor Mian Zhang, Department of Medicinal Plants, China

103 Pharmaceutical University, Nanjing, China.

104 2.2 Experimental animals

105 Adult female and male Sprague-Dawley rats (250±20 g), were purchased from

106 Comparative Medicine Center of Yangzhou University (Yangzhou, China). The rats

107 were reared on a 12/12 h light/dark cycle at 25±2 °C and allowed free access to water

108 and standard chow ad lib. Animals were reared and handled strictly according to the

109 obligations of the Animal Ethics Committee of China Pharmaceutical University and

110 the guidelines for the Care and Use of laboratory animal from the National Institute of

111 Health. The animals were acclimated for 10 days prior to operation.

112 2.3 Drug administration and MCAO model construction

113 Rats were randomly selected and assigned to eight groups (≥20 rats each): (1) the

114 female sham-operated group (NF), (2) the male sham-operated group (NM), (3) the

115 female MCAO model group (MF), (4) the male MCAO model group (MM), (5) the

116 female HLJDD-treated group (TF), (6) the male HLJDD-treated group (TM), (7) the

117 female negative control group (HF), and (8) the male negative control group (HM).

118 The rats in sham operation and MCAO model groups received vehicle (0.5 %

119 CMC-Na), HLJDD treated and negative control groups received HLJDD (5 g per kg

120 per day, weight ratio between crude drug and rat). The drug and vehicle were orally

121 administrated once a day for 10 consecutive days. After 12 h fasting, the MCAO

122 model was established at day eleven by ligating the right middle cerebral artery. The

123 operation procedures were achieved according to the methods of Longa et al. [33] and

124 Nagasawa and Kogure[34] with slight modification, as described in our previous report.[31]

125 The animals were anesthetized with 3.5 % chloral hydrate (350 mg/kg body weight)

126 and fixed onto a pad. Then, arteries separation was undergone, the arteriotomy hole

127 made between the right external carotid artery (ECA) stump and the carotid

128 bifurcation, and a poly lysine coated nylon monofilament was inserted, nearly 18-20

129 mm, through the ipsilateral internal carotid artery (ICA) to obstruct the blood flow into

130 the middle cerebral artery (MCA), to achieve cerebral ischemia. Two hours later,

131 twenty-four hours reperfusion was followed by gently pulling out the filament. The

132 same operation was performed on the sham group and negative control surgery rats,

133 except for filament insertion.

134   2.4 Sample collection

135   After 24 hours reperfusion, behavioral changes were assessed to evaluate neural

136   function. The rats were deeply anesthetized with 3.5 % chloral hydrate and then

137   sacrificed, after which blood, cerebrum and cerebellum tissues were collected rapidly.

138   Blood was collected from the abdominal aorta, and serum samples were obtained by

139   centrifugation (12,000 rpm, 10 min, 4 °C) and stored at -80 °C before analysis.

140   Cerebrum and cerebellum tissues were quickly removed, weighed, and rinsed with

141   cold phosphate-buffered saline (PBS). The cerebrums for histological and

142   immunohistochemical examination in each group were fixed in 10 % neutral buffered

143   formalin. Half of the right (ipsilateral to MCAO) cerebral hemispheres, and

144   cerebellums were frozen and stored at -80 °C for ^{1}H NMR recording. The other half of

145   the right hemispheres were stored at -80 °C before the measurement of oxidative

146   stress-related biological parameters and mitochondrial energy metabolism related

147   enzymes, including nitric oxide (NO), malondialdehyde (MDA), glutathione (GSH),

148   glutathione disulfide (GSSG), superoxide dismutase (SOD), glutathione peroxidase

149   (GSH-PX), Ca^{2+}-ATP enzyme and Na^+/K^+-ATP enzyme. (All assay kits purchased

150   from Nanjing Jiancheng Bioengineering Institute, Nanjing, China).

151   2.5 Neurobehavioral abnormality evaluation

152   Neurobehavioral dysfunction of rats in the eight groups (n=10 in each group) was

153   estimated by observers blind to the experiment using Longa's[33] five-point scale: 0,

154   normal (no neurobehavioral dysfunction); 1 slight (failure of flexing left forepaw

155   fully); 2 moderate (circling counterclockwisely); 3 severe (leaning to the affected side);

156   and 4 very serious (no autonomous activity and unconsciousness).

157   2.6 Evaluation of cerebral infarct volume

158   Cerebral infarct volumes were measured with 2, 3, 5-triphenyltetrazolium chloride

159   (TTC) staining and used to describe the severity of cerebral ischemia. Cerebrums were

160   sliced into 6 uniform 2-mm thick coronal sections, stained with 1 % TTC, and

161   incubated at 37 °C for 30 min in the dark, then fixed in 10 % neutral buffered formalin

162   overnight. After staining with TTC, normal region of tissue was stained in a rose red

163   color, and the infarct region of tissue was stained in white.[32] Slices stained with TTC

164   were photographed, and analyzed by image analysis software (Image-Pro Plus 6.0).

165   For each sample, the total infarction and slice volume were the sum of the results of

166   the six slices, and then the infarction volume ratio was calculated as dividing the total

167   infarction area by the total slice area. The kit of TTC, was bought from Nanjing

168   Jiancheng Bioengineering Institute (Nanjing, China).

169   2.7 Histopathological assessment by H&E Staining

170   Fresh rat cerebrums were quickly removed, rinsed with cold phosphate buffered

171   saline (PBS), immersed in 10 % neutral buffered formaldehyde for 24 h, and then

172   embedded in paraffin. A series of adjacent 5-µm-thick sections were cut from the

173   coronal plane of the cerebrum, stained with hematoxylin and eosin (H&E) and

174   examined by light microscopy (200×).

175   2.8 Immunohistochemistry

176   Serial 3 µm thickness of sections of formalin-fixed, paraffin-embedded cerebrum

177   tissues were used for immunohistochemistry as previously described.[21] The activity of

178 caspase-3, glial fibrillary acidic protein (GFAP), p65 and vascular endothelial growth

179 factor (VEGF) were evaluated by Goodbio technology CO., LTD (Nanjing, China).

180 Each experiment was performed for at least three times. The staining was

181 photographed under light microscopy, and analyzed by image analysis software

182 (Image-Pro Plus 6.0).

183 2.9 Sample preparation for ^{1}H NMR spectroscopic analysis

184 2.9.1 ^{1}H NMR spectroscopy of serum samples

185 After thawing, serum samples (300 μl) were added to 150 μl of buffer solution (0.2

186 mol/l Na_2HPO_4 and 0.2 mol/l NaH_2PO_4, pH 7.4) and 150 μl of TSP

187 (3-trimethylsilylpropionic acid, 1 mg/ml, Sigma-Aldrich) in D_2O. D_2O was used for

188 field frequency locking, TSP was used as the chemical shift reference ($\delta_H = 0.00$ ppm),

189 and phosphate buffer was added to minimize the chemical shift variation due to

190 differences in the pH discrepancy of samples. After vortexing, the mixture was

191 allowed to stand for 20 min and then centrifuged at 12,000 rpm for 10 min at 4 °C to

192 remove any precipitate. Aliquots of 550 μl of the supernatant were placed into 5-mm

193 NMR tubes.

194 All ^{1}H NMR spectra were recorded at 25 °C on a Bruker AV 500 MHz spectrometer.

195 A water-suppressed Carr-Purcell-Meibom-Gill (CPMG) spin-echo pulse sequence

196 (90(τ-180-τ)n-acquisition) with a total spin-echo delay (2 nτ) of 10 ms was used to

197 suppress broad signals from macro molecules (i.e., proteins or lipoproteins),

198 whereupon the signals of micro molecules were clearly observed. ^{1}H NMR spectra

199 were measured with 128 scans producing 32,000 data points over a spectral width of

200 7,500 Hz.[40] The spectra were Fourier transformed after multiplication by an

201 exponential window function with a line broadening of 0.5 Hz and were then manually

202 phased and baseline corrected.

203 2.9.2 ^{1}H NMR spectroscopy of cerebrum and cerebellum extracts

204 Pre-weighed cerebrum and cerebellum tissues (200 mg) were homogenized in 50 %

205 acetonitrile/H$_2$O (1.5 ml) and centrifuged at 12,000 rpm for 10 min at 4 °C. The

206 supernatant was collected, lyophilized and reconstituted in 600 μl D$_2$O (0.2 mol/l

207 Na$_2$HPO$_4$ and 0.2 mol/l NaH$_2$PO$_4$, pH 7.4, containing 0.05 % TSP). All mixed samples

208 were vortexed, and allowed to stand for 20 min prior to centrifugation at 12,000 rpm

209 for 10 min at 4 °C to remove any precipitates. The collected supernatants, ca. 550 μl,

210 were then pipetted out into a 5 mm NMR tube.

211 ^{1}H NMR data of the cerebrum and cerebellum extracts were recorded on a Bruker

212 Avance spectrometer operating at 500 MHz. To suppress residual water, a nuclear

213 overhauser enhancement spectroscopy (NOESY) pulse sequence (relaxation

214 delay-90°-μs-90°-tm-90°-acquire-FID) was applied. The water signal is suppressed

215 using noise irradiation during the recycle delay and the NOESY mixing time.

216 Typically, 128 free induction delays (FIDs) were collected into 32K data points, using

217 a spectral width of 10 kHz, an acquisition time per scan of 2.54 s, recycle delay of 2 s

218 and a mixing time of 100 ms. Prior to Fourier transformation, an exponential

219 line-broadening function of 0.3 Hz was applied to the FID. All ^{1}H NMR spectra were

220 manually phased and baseline corrected.

221 2.10 Data processing

222   The processing methods used on the raw NMR data were based on protocols

223   described in our previous work.[41] Briefly, all ^{1}H NMR spectra were manually phased,

224   baseline corrected, referenced to TSP (1H, δ 0.00) using Bruker Topspin 3.0 software

225   (Bruker GmbH, Karlsruhe, Germany), automatically exported to ASCII files using

226   MestReNova (Version 8.0.1, Mestrelab Research SL, Santiago de Compostela, Spain),

227   and then imported into "R" (http://cran.r-project.org/). The data were aligned further

228   with an R script developed in-house. The spectra were then binned into 0.015 ppm

229   integrated spectral buckets between 0.2 and 10 ppm. Regions of residual water

230   resonances (4.65 to 5.25 ppm for cerebrum and cerebellum extracts, and 4.70–9.70 for

231   serum) were removed to avoid their interference.[41] The integral values of each

232   spectrum were then probability quotient normalized to account for different sample

233   dilutions.

234   2.11 Multivariate analysis

235   The data were mean-centered and Pareto-scaled before multivariate analysis.

236   Non-supervised principal components analysis (PCA) was first used to see the

237   separation trend of groups. However, no obvious clustering was observed (data not

238   shown). Supervised orthogonal signal correction partial least-squares discriminant

239   analysis (OSC-PLS-DA) was then carried out to disclose the metabolic differences

240   between the classes, filtering out effects that were unrelated to grouping. Repeated

241   two-fold cross-validation (20 times) method and permutation test were applied in the

242   OSC-PLS-DA model; the validity of the models against overfitting was assessed by

243   the parameter R^2, and the predictive ability was described by Q^2.

244   2.12 Univariate analysis

245   Parametric (Student's t-test) or non-parametric Mann-Whitney statistical test

246   (depending on conformity to the normal distribution) was performed to validate

247   important metabolites that were increased or decreased between groups using R. The

248   fold change values of metabolites between groups were calculated.[45] The Benjamini &

249   Hochberg method[35] was used to adjust the related p-values for controlling the false

250   discovery rate in multiple comparisons applying scripts written in R language, which

251   is available freely, open-source software package.

252

253   **3. Results**

254   3.1 Mortality

255   Mortalities from MCAO were 58.2 % (32/55) for female rats and 64.7 % (22/34) for

256   male rats. HLJDD greatly reduced the mortalities arising from MCAO to 30.0 % (6/20)

257   for female rats and 40.0 % (8/20) for male rats (Fig 1A).

258   3.2 Neurobehavioral abnormality scoring

259   The neurological damage was evaluated by an observer blind to the experiment

260   using a five-point scale. The score was 0.67 ± 0.62 for TF group (HLJDD-treated

261   females) vs. 1.4 ± 0.64 for MF group (MCAO females rats), and 1.2 ± 0.69 for TM group

262   (HLJDD-treated males) vs. 2.1 ± 0.49 for MM group (MCAO males) (Fig. 1B).

263   3.3 Cerebral infarct volume

264   The coronal infarct volume (mean$\pm$S.D.) was 39.5 ± 1.4 % for female rats, and

265   46.0 ± 2.0 % for male rats. HLJDD could significantly reduce the infarct area of

266 cerebral ischemia-reperfusion (CI/R) to 17.9$\pm$2.0 % in females, and 25.1$\pm$1.4 % in

267 males according to the TTC staining of cerebral slices (Fig. 1C and D).
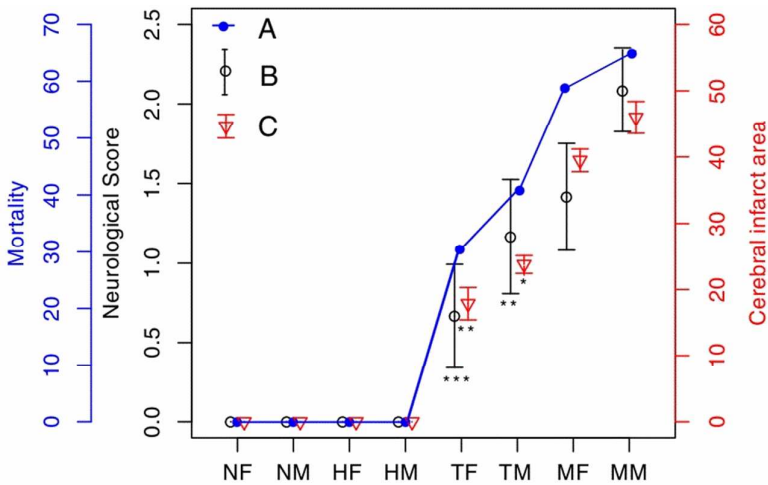

268
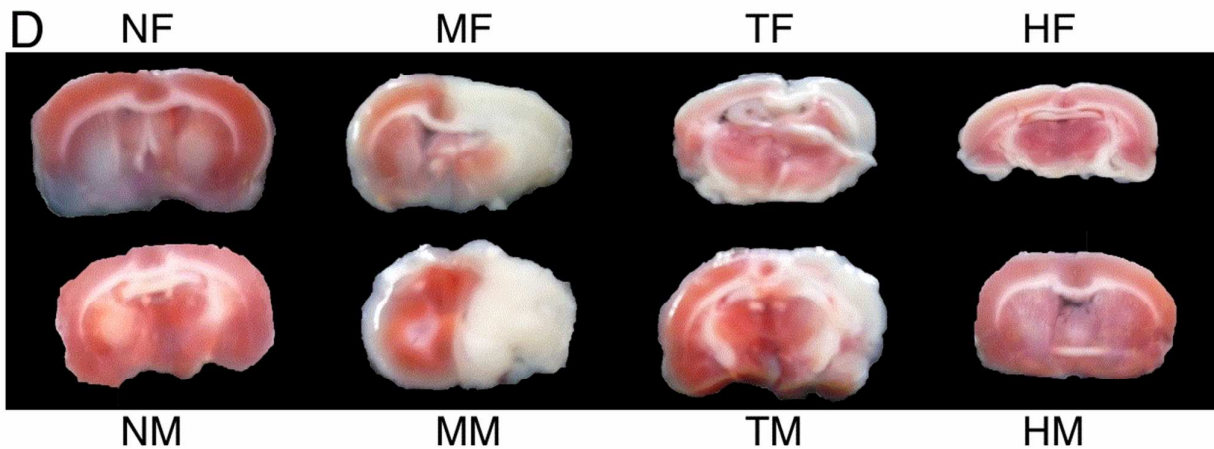
269

270 **Fig. 1** Rats, in the model and HLJDD treated groups, experienced a 2 h ischemia, followed by 24 h reperfusion
271 using the middle cerebral artery occlusion (MCAO) model. Neurological disability of rats was then assessed and
272 brain tissues were collected for TTC staining. (A) Mortality of the model and HLJDD treated groups; (B)
273 Neurobehavioral scores of the model and HLJDD treated groups; (C and D) Infarct regions restored by HLJDD
274 pretreatment, revealed by TTC (2,3,5-triphenyltetrazolium chloride) staining: infarct area (C), TTC staining of
275 brain (D). Data obtained were expressed as mean$\pm$standard deviation (S.D.), n>10. ***: P< 0.001, **: P< 0.01
276 HLJDD treated groups vs. MCAO group, indicating a better therapeutical effect of HLJDD for females than males.

277 3.4 Histopathological assessment

278   Compared with the sham groups (Fig. 2A and 2E), healthy rats administered with

279 HLJDD (negative control groups) exhibited no pathological changes (Fig 2D and 2H).

280 Apparent pathological changes occurred in cerebrum tissue of MCAO rats: liquefied

281   changes and polynesic sponginess in brain tissue, swelled degeneration of glial cells,

282   and disordered arrangement of neurons and shrinked nucleus (Fig 2B and 2F). In

283   HLJDD treated rats, these abnormalities in females were more successfully alleviated

284   than males (Fig. 2C and 2G).
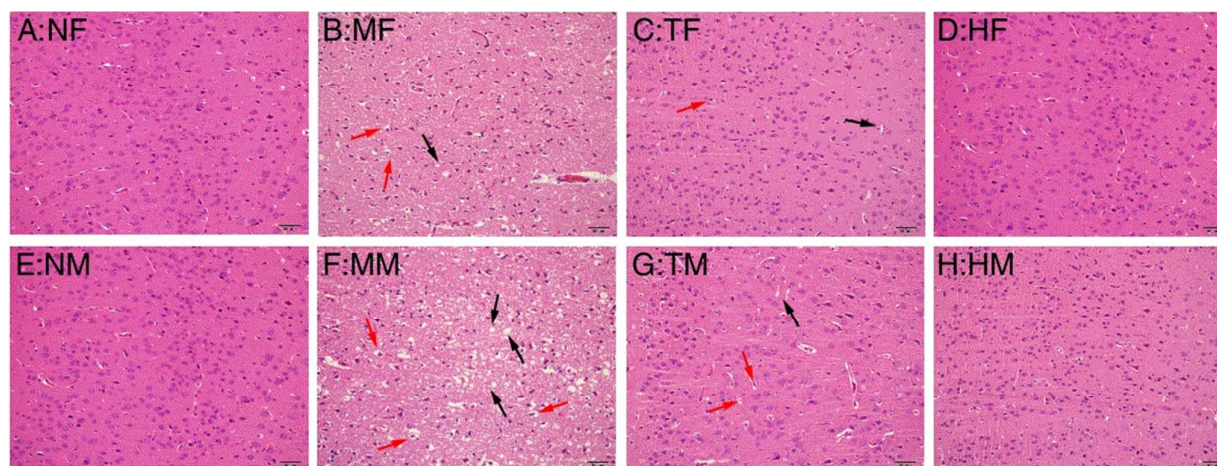
286   **Fig. 2** Photomicrographs of sections of female brain tissues (A-D) and male brain tissues (E-H) taken at 200 x
287   magnification. (A, E) Normal brain cytoarchitecture; (B, F) Pathological abnormality in MCAO groups; (C, G);
288   Pathological changes in the brain after the administration of HLJDD; (D, H) Physiological cytoarchitecture of the
289   brain in negative control groups. Tissue or cells in MCAO groups were apparently abnormal: liquefied changes and
290   polynesic sponginess in brain tissue (red arrow), glial cells of swelled degeneration, disordered neurons
291   arrangement (black arrow).

292   3.5 Immunohistochemical analysis

293   Compared with sham groups (Fig. 3A1-2, 3B1-2, 3C1-2 and 3D1-2), the positive

294   cells expression of caspase-3, GFAP, p65 and VEGF are significantly increased in

295   MCAO groups (Fig. 3A 3-4, 3B 3-4, 3C 3-4 and 3D 3-4). HLJDD notably reduced the

296   levels of caspase-3, GFAP, p65 and VEGF activity in the ischemic stroke by 28.4 %,

297   38.7 %, 26.5 % and 31.2 %, respectively (Fig. 3A 5-6, 3B 5-6, 3C 5-6, 3D 5-6, E, F, G,

298   and H). There were no noticeable difference in negative control groups from the sham

299   groups (Fig. 3A 7-8, 3B 7-8, 3C 7-8 and 3D 7-8).

300

301
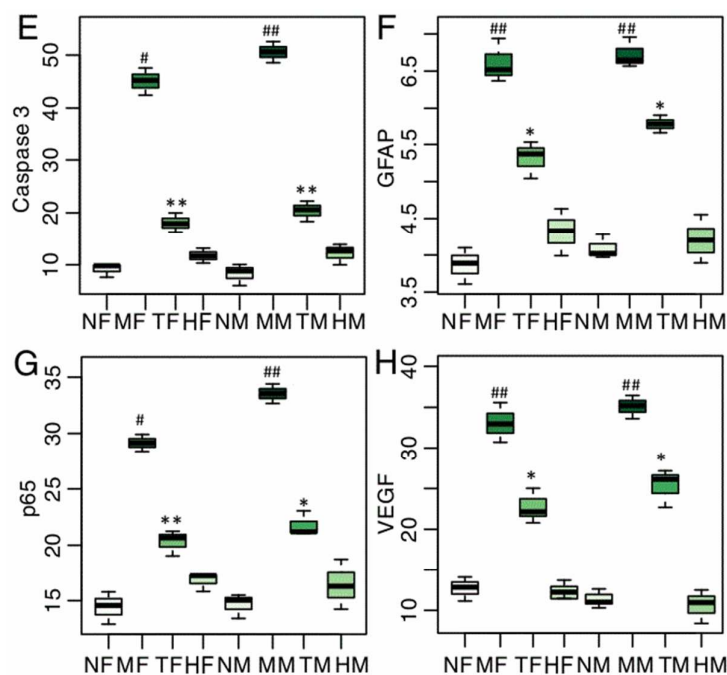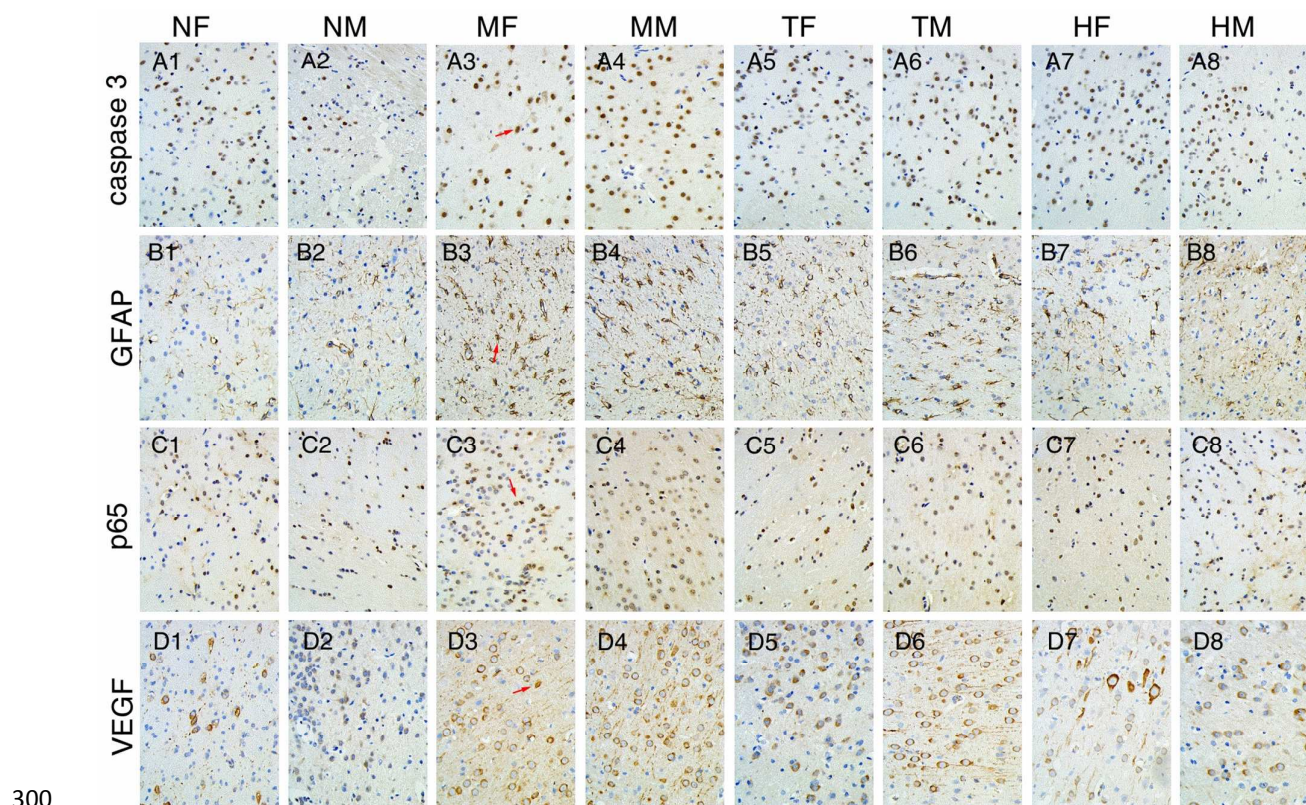
Fig. 3 After subjected to ischemia (2h) and reperfusion (24 h), the brain tissue proteins were harvested for measuring caspase-3 (A1-8, x400), GFAP(B1-8, x400), p65 (C1-8, x400) and VEGF (D1-8, x400) activitives by immunohistochemistry as described in Section 2. N=3 in each group; (E, F, G, H) The mean integrated optical density (IOD) was calculated as a protein expression quantity of positive cell (red arrow). Values are means ± S.D. Bars with different superscript letters are significantly differentiation from each other ([#]$P < 0.05$ and [##]$P < 0.01$

307   MCAO group vs. sham group, and *P < 0.05, while ** P < 0.01, HLJDD treated groups vs. MCAO group).

308   3.6 Biochemical analysis

309   The biochemical parameters in different groups were shown in Fig. 4. The levels of

310   NO and MDA (Fig. 4A and B), the oxidative stress markers, exhibited a significant

311   increase in the model group (p<0.05) compared with the sham group both in female

312   and male rats. HLJDD treatment significantly decreased the enhanced levels of NO

313   and MDA in model rats. The model groups had a notable reduction in the quantity of

314   GSH (Fig. 4C), and a significant accumulation of GSSG (Fig. 4D), which could also

315   be significantly reversed by HLJDD. The activities of antioxidase GSH-PX and SOD

316   (Fig. 4E and F) were significantly inhibited in model groups compared with the sham

317   groups, which were greatly reversed by HLJDD. Moreover, HLJDD markedly

318   enhanced the activities of Na^+/K^+-ATPase and Ca^{2+}-ATPase (Fig. 4G and H), which

319   were significantly inhibited in the model groups.
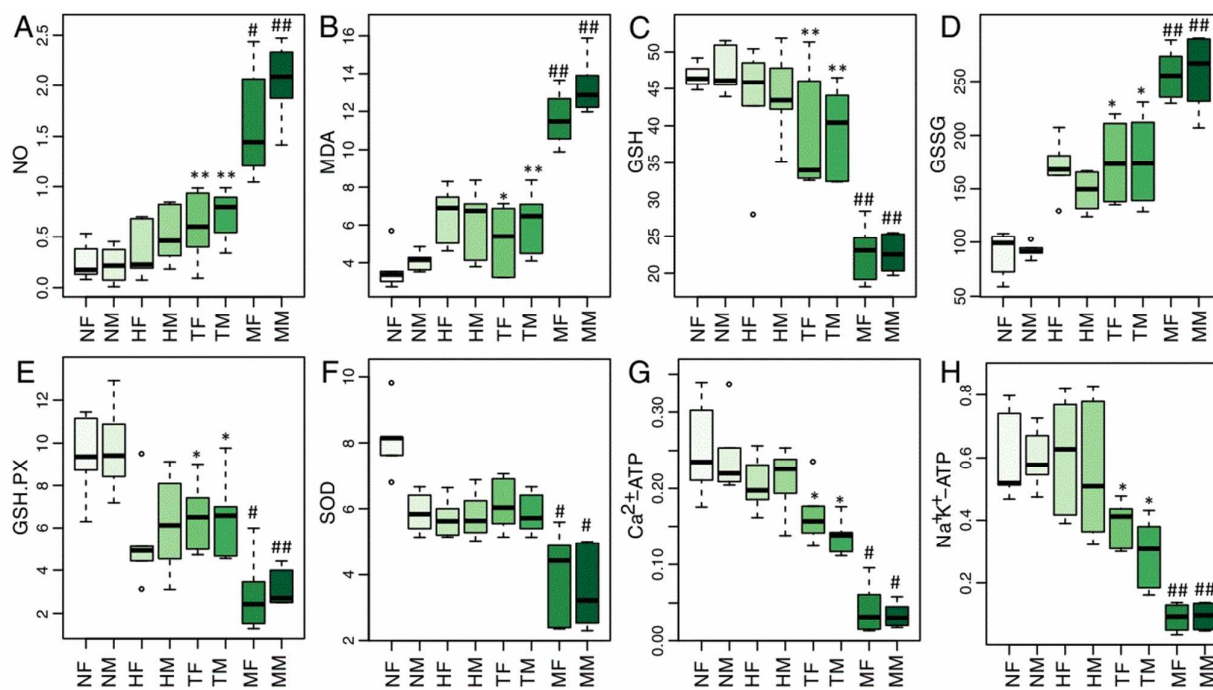
320

321 **Fig. 4** Boxplots for values of NO (A), MDA (B), GSH (C), GSSG (D), GSH-PX (E), SOD (F), Ca^{2+}-ATP enzyme
322 (G) and Na^{+}-K^{+}-ATP enzyme (H) in each group. At the bottom of each box, the line drawn in the box and at the top
323 of the box represent the 1st, 2nd, and 3rd quartiles, respectively. The whiskers extend to $\pm$ 1.5 times the
324 interquartile range (from the 1st to 3rd quartile). Outliers are shown as an open circle. All the values are mean $\pm$
325 S.D. (n > 6). #: $P < 0.05$ and ##$P < 0.01$ MCAO group vs. sham group, hinting a successful model established. *:
326 HLJDD treated groups vs. MCAO group, and $P < 0.05$, while ** $P < 0.01$, suggesting a good efficacy of drug
327 treatment.

328 3.7 Metabolites identified in ^{1}H NMR spectra of serum and tissue

329   Typical ^{1}H NMR spectra for serum, cerebrum extract and cerebellum extract of rats

330 were presented in Fig. 5, with major metabolites labeled. The signals were assigned by

331 querying publicly accessible metabolomics databases,[47] such as Madison

332 (http://mmcd.nmrfam.wisc.edu/), MMCD (http://mmcd.nmrfam.wisc.edu/), ECMDB

333 (http://www.ecmdb.ca/) and HMDB (http://www.hmdb.ca/) aided by Chenomx NMR

334 suite. The detailed information of the metabolites was listed in Tables S1, S2 and S3.
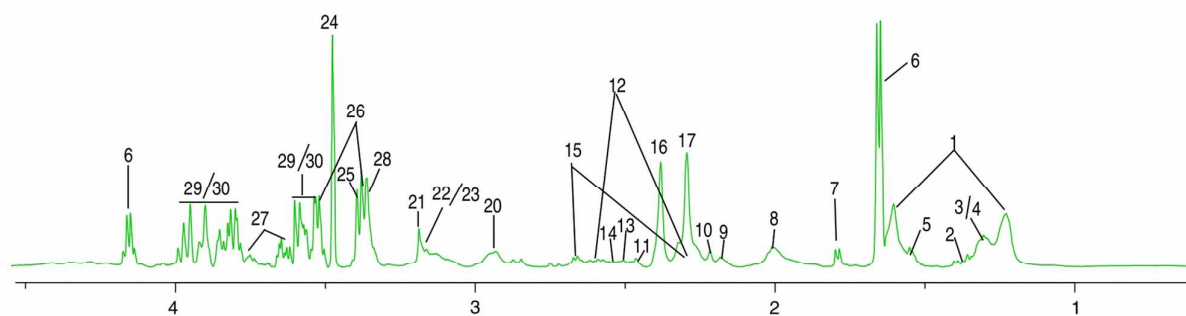
335
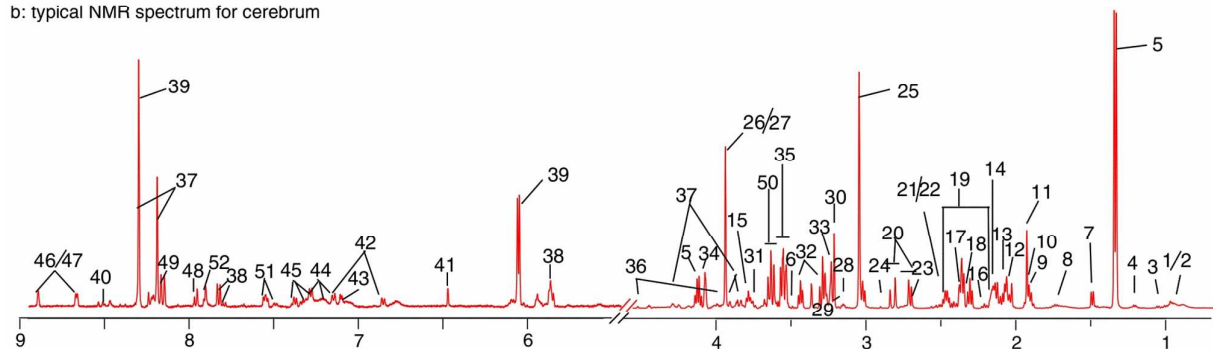
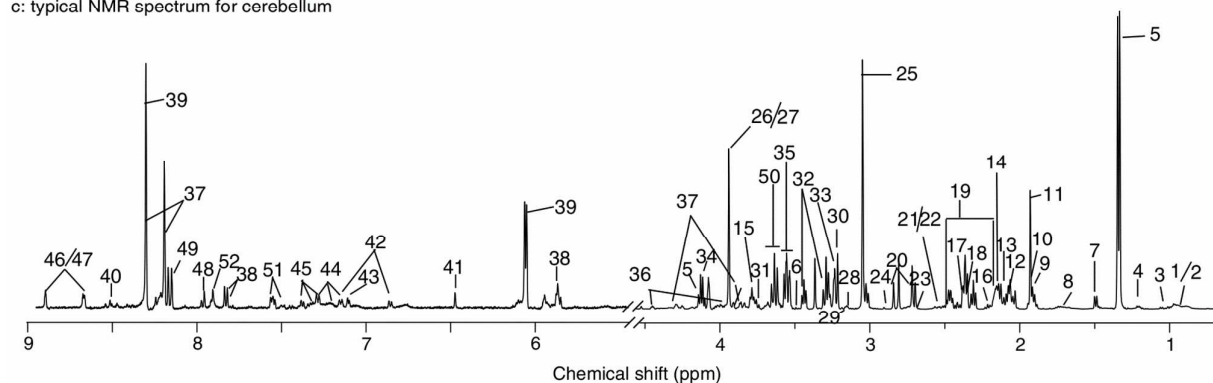**Fig. 5** Typical 500 MHz ^{1}H NMR s pectra of serum (a), brain (b), and cerebellum (c) obtained from the sham, the MCAO, the HLJDD-treated and the negative control groups. Metabolites in serum: 1, LDL/VLDL; 2, Valine (Val); 3, Leucine (Leu); 4, Isoleucine (Ile); 5, β-Hydroxybutyrate (3-HB); 6, Lactate (Lac); 7, Alanine (Ala); 8, Lysine (Lys); 9, Arginine (Arg); 10, Acetone (Ace); 11, Acetoacetate (Acet); 12, Glutamate (Glu); 13, Pyruvate (Pyru) ; 14, Succinate (Suc); 15, Glutamine (Gln); 16, O-Acetyl Glycoproteins (OAG); 17, N-Acetyl Glycoproteins (NAG); 18, Citrate (Cit); 19, Isocitrate (Isoc); 20, PUFA; 21, Creatinine (Cre); 22, Creatine (Cr); 23, phosphocreatine (PCr); 24, Methanol (MeOH); 25, TMAO; 26, Taurine (Tau); 27, Glycerol (Gyo); 28, Betaine (Bet); 29, β−Glucose (β−Glc); 30, a-Glucose (a-Glc). Metabolites in cerebrum and cerebellum tissues:1, Ile; 2, Leu; 3, Val; 4, 3-HB; 5, Threonine; 6, Lac; 7, Ala; 8, Lys; 9, Arg; 10, γ-amino-butyrate (GABA); 11, Acetate (AC); 12, N-acetylaspartic acid (NAA); 13, Methionine (Met); 14, Glu; 15, Glutathione (GSH); 16, Ace; 17, Pyr; 18, Suc; 19, Gln; 20, Asparate (Asp); 21, Cit; 22, Isoc; 23, Mal; 24,Trimethylamine (TMA); 25, Cre; 26, Cr; 27, PCr; 28, Ethanolamine (ETA); 29, choline (Cho); 30, O-phosphocholine (OPC); 31, Glc; 32, Tau; 33, Bet; 34, Myo-inositol (Myo); 35, Glycine (Gly); 36, Ascorbate (Asc); 37,Inosine (Ino); 38, Uridine (UDP); 39, Adenosine (Ade); 40, AMP; 41, Fumarate (Fum); 42, Tyrosine (Tyr); 43, Histidine (His); 44, Tryptophan (Trp); 45, Phenylalanine (Phe); 46, Nicotinamine; 47,

350 Nicorinurate (Nic); 48, 3-Methylxanthine (3-MX); 49, Hypoxanthine (Hyp); 50, Gyo; 51, Uracil (Ura), 52,

351 Xanthine (Xan).

352 3.8 Multivariate analysis of ^{1}H NMR spectral data of all groups

353 The ^{1}H NMR data from the sham, the MCAO, the HLJDD-treated and negative

354 control rats were evaluated using OSC-PLS-DA analysis to investigate the treatment

355 of HLJDD. In the score plots, the showcased clusters correspond to metabolic patterns

356 in different groups with each point representing one sample. In the OSC-PLS-DA

357 score plots (Fig. 6a) of female rats (NF, MF, TF, HF), the four groups were aligned

358 according to HLJDD administration, those treated with HLJDD (TF and HF) were on

359 the left, those not on the right, with the MF and NF groups overlapping with each

360 other, which suggested that HLJDD produced stronger influences on the metabolic

361 profiles of female rats than MCAO injury. In contrast, the OSC-PLS-DA score plots

362 (Fig. 6b) of male rats (NM, MM, TM, HM) showed a predominance of the influence

363 of MCAO model than that of HLJDD: the groups with MCAO modelling were on the

364 left, and those not on the right. An explanation for the dramatic differences observed in

365 serum between female and male remains unknown, although differences in hormones,

366 hormone receptors, and enzyme concentrations may play a contributing role. The

367 OSC-PLS-DA score plots for cerebrum extracts (Fig. 6c) showed clear separation of

368 MCAO groups from sham groups, suggesting a severe metabolic perturbation induced

369 by MCAO. HLJDD-treated groups were in the middle of the MCAO and sham groups.

370 As illustrated by the score plots (Fig. 6d), female rats after MCAO modelling were on

371 the left, separated from those of the sham and negative control groups, with

372 HLJDD-treated group in between. However, HLJDD-treated group and MCAO model

373   group were partially overlapped for male rats (Fig. 6e). In the scores plots of Fig. 6f,

374   the female MCAO model group and female HLJDD-treated group were the furthest

375   away from each other, with the male groups (MM and TM) in the middle, partially

376   overlapped. These results suggested a better therapeutic effect of HLJDD on MCAO

377   females than males, in consistent with the pathological and neurobehavioral

378   observations.

379
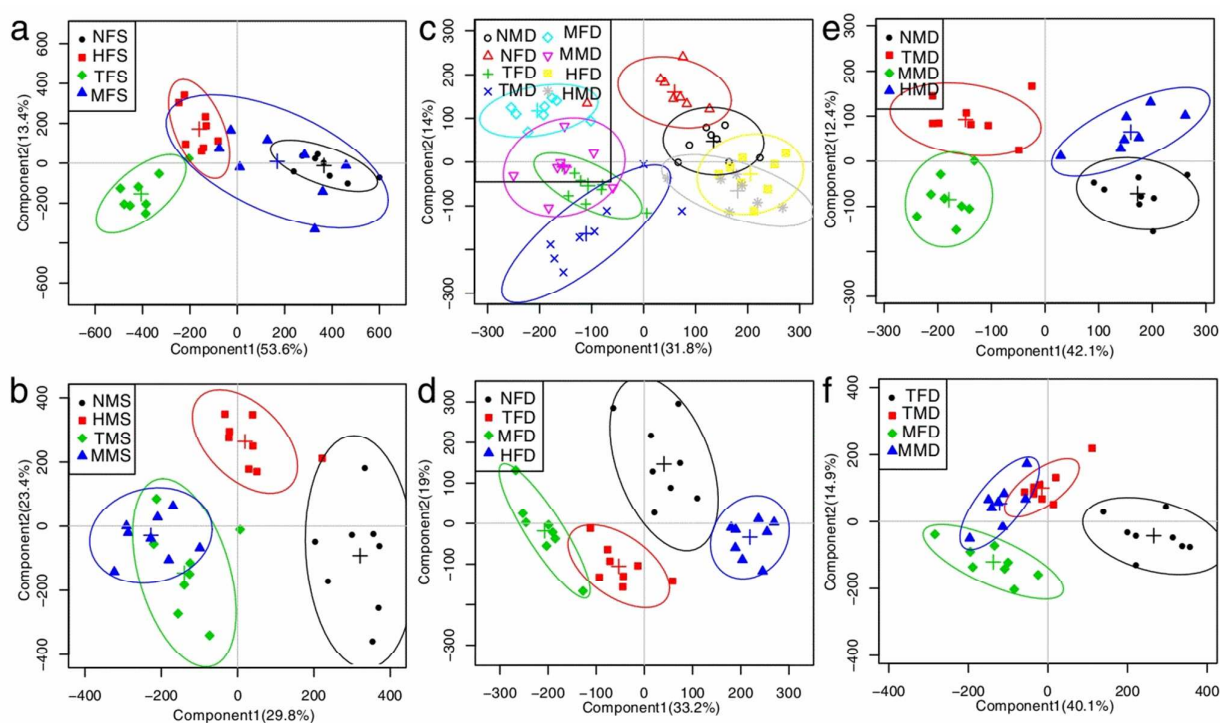
380   **Fig. 6** Score plots for OSC-PLS-DA analysis based on ^{1}H NMR spectra of serum and cerebrum extracts obtained
381   from the sham, the MCAO, the HLJDD-treated and the negative control rats. Two independent analyses were
382   performed to study the female (NF, MF, TF, and HF) (a and d) and male (NM, MM, TM, and HM) (b and e)
383   relationships of the HLJDD treatment. (a, b) score plots for serum OSC-PLS-DA analysis; (c, d, e, f) score plots for
384   cerebrum extracts OSC-PLS-DA analysis. OSC-PLS-DA score plots exhibit distinct distributions of metabolites
385   and are capable of gender dependently distinguishing HLJDD-administered rats from the MCAO and the control
386   group.

387   3.9 Metabolic changes in MCAO and HLJDD-treated rats

388   The OSC-PLS-DA score plots analysis above investigated the effects of HLJDD to

389   females and males. To further explore the metabolic events happened in MCAO and

390   find out metabolites that were directly associated with the treatment effects of HLJDD,

391   the NMR data of these MCAO and HLJDD-treated groups were compared with that of

392   sham and MCAO by OSC-PLS-DA analysis, individually.

393   3.9.1 Metabolic changes in serum of MCAO rats

394   NM and MM group showed well separation ($R^2Y = 0.92$ and $Q^2Y = 0.78$, Fig. 7g) in

395   the score plots of OSC-PLS-DA analysis of serum NMR data (Fig. 7a). The

396   contribution of metabolites to the separation of the two groups were visualized by the

397   loading plots (Fig. 7b), color-coded according to the absolute value of correlation

398   coefficients, and presented in a covariance-based pseudo-spectrum,[36, 37] a hot-colored

399   signal (red) indicates more significant contribution to the class separation than a

400   cold-colored one (blue). Considering both the covariance (X axis) and correlation (Y

401   axis) between metabolites and the modeled class designation, the S-plot (Fig. 7e),

402   another way of displaying loadings data, was used to identify potentially significant

403   metabolites, being placed in the lower left and upper right quadrant and farther away

404   from the origin. The upper section of color-coded loading plots and S-plot indicate that

405   the designated metabolites are present at lower concentration: 3-HB, alanine,

406   glutamine, TMAO, acetoacetate, citrate, betaine, creatine, PCr, pyruvate and glucose;

407   whereas the low section represented metabolites increased: LDL/VLDL, leucine,

408   isoleucine, lactate, lysine, valine, choline, OPO, NAG, OAG, PUFA, arginine and

409   taurine.
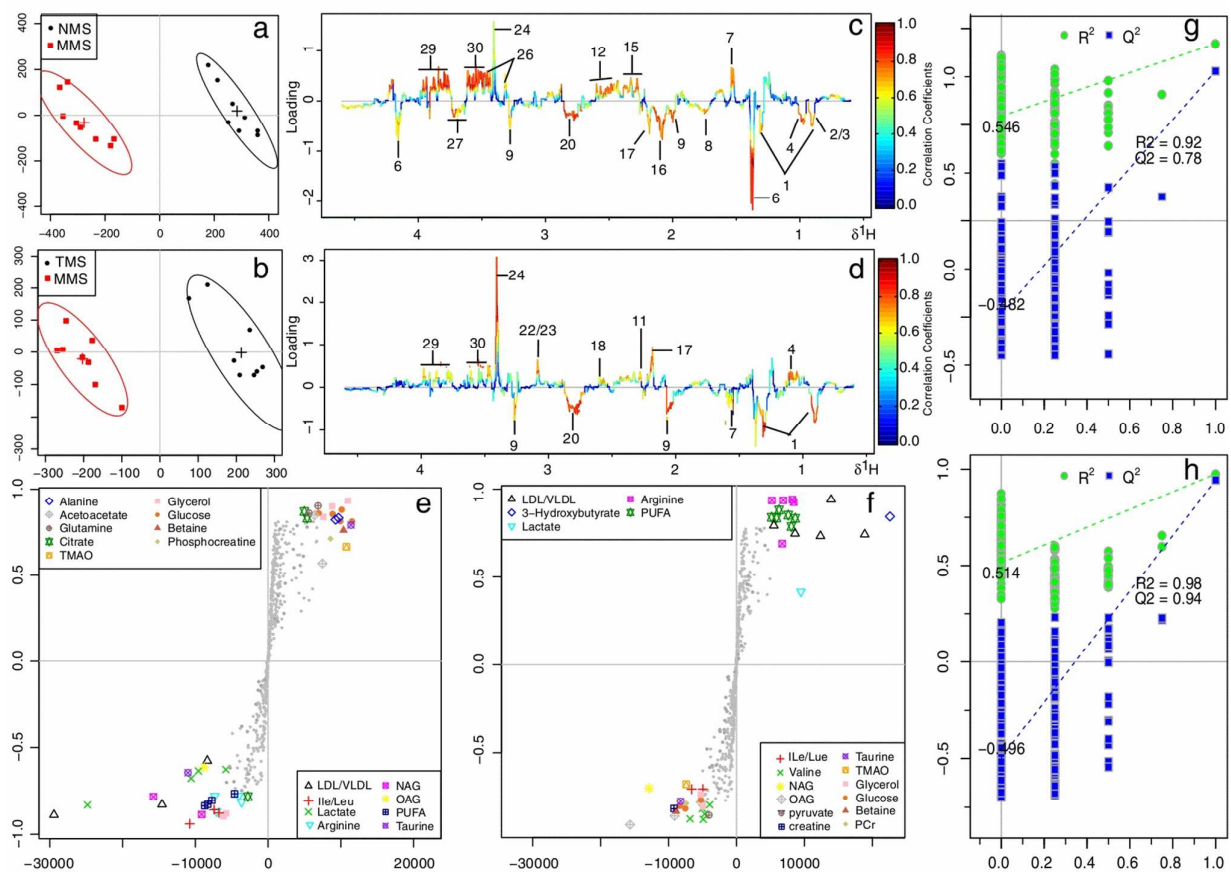
Fig. 7 OSC-PLS-DA analysis of serum samples ^{1}H NMR dataset of NM, MM and TM groups. Scores plots (a and c) and the loading plots of OSC PLS-DA (b and d) were analyzed after the removal of H_2O signals. Metabolite variation was visualized by the loading plots, which are color-coded according to the absolute value of the correlation coefficient; a red signal indicates a more significant contribution to the class separation than a blue signal. Positive peaks indicate a relatively decreased metabolite level in dosed groups, while negative peaks indicate an increased metabolite level in HD group. Metabolites: 1, LDL/VLDL; 2, Val; 3, Leu; 4, Ile; 6, Lac; 7, Ala; 8, Lys; 9, Arg; 11, Acet; 12, Glu; 15, Gln; 16, OAG; 17, NAG; 18, Cit; 20, PUFA; 22, Cr; 23, PCr; 24, MeOH; 26, Tau; 27, Gyo; 29, β–Glc; 30, a-Glc. Color-coded S-plots for OSC-PLS-DA analysis of ^{1}H NMR data in serum (e, f) for N, M and HLJDD administrated male rats. OSC-PLS-DA scatter plot from serum (g and h) of the statistical validations obtained by 200 times permutation tests, with R^2 and Q^2 values in the vertical axis, the correlation coefficients (between the permuted and true class) in the horizontal axis, and OLS line representing the regression of R^2 and Q^2 on the correlation coefficients.

3.9.2 Metabolic changes in cerebrum and cerebellum of MCAO rats

424   3.9.2.1 Female rats

425   The NF and MF showed good separation ($R^2Y = 0.97$ and $Q^2Y = 0.86$ for cerebrum,

426   and $R^2Y = 0.90$ and $Q^2Y = 0.80$ for cerebellum, respectively) (Fig. 11a and e) in the

427   scores plots for OSC-PLS-DA analysis of NMR data from cerebrum tissue and

428   cerebellum tissue (Fig. 8a and 9a). The loading plots (Fig. 8b and 9b) and S-plots (Fig.

429   10a and c) revealed that in MF samples: acetate, creatinine, alanine, lysine, acetone,

430   succinate, malate, AMP, citrate, NAA, isocitrate, betaine, glycerol, myo-inositol,

431   lactate, histidine, serine, adenosine decreased in cerebrum, 3-HB, acetate, taurine,

432   inosine, serine, GSH, AMP, asparate, pyruvate and acetone decreased in cerebellum.

433   Whereas the low section represented that the designated metabolites are present at

434   higher concentrations in MF samples on average: leucine, isoleucine, valine, glutamate,

435   GABA, taurine, glycine, acetate, NAA, GSH, creatinine, tyrosine, tryptophan,

436   phenylalanine, pyruvate, betaine and glutamine increased in cerebrum, leucine,

437   isoleucine, alanine, choline, OPC, lysine, NAA, glycine, myo-inositol, glycerol,

438   tyrosine, phenylalanine and creatinine increased in cerebellum.
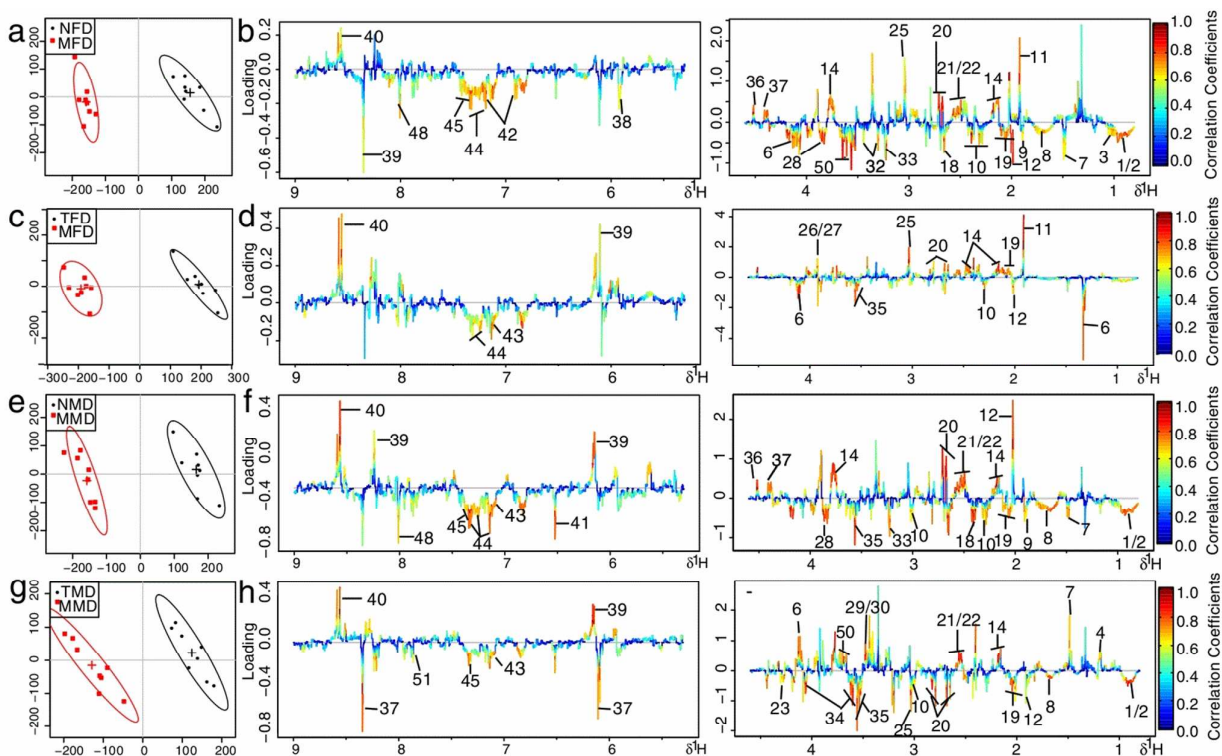
439

440 **Fig. 8** OSC-PLS-DA analysis of cerebrum extracts ^{1}H NMR dataset of NF, MF, TF, NM, MM, and TM. Score plots

441 (a, c, e and g) and the loading plots of OSC-PLS-DA (b, d, f and h) were analyzed after the removal of H_2O signals.

442 Metabolite variation was visualized by the color-coded loading plots. Metabolites: 1, Ile; 2, Leu; 3, Val; 4, 3-HB; 6,

443 Lac; 7, Ala; 8, Lys; 9, Arg; 10, GABA; 11, AC; 12, NAA; 14, Glu; 18, Suc; 19, Gln; 20, Asp; 21, Cit; 22, Isoc; 25,

444 Cre; 26, Cr; 27, PCr; 28, ETA; 29, Cho; 30, OPC; 32, Tau; 33, Bet; 34, Myo; 35, Gly; 36, Asc; 37, Ino; 38, UDP;

445 39, Ade; 40, AMP; 41, Fum; 42, Tyr; 43, His; 44, Trp; 45, Phe; 48, 3-MX; 50, Gyo; 51, Ura.

446
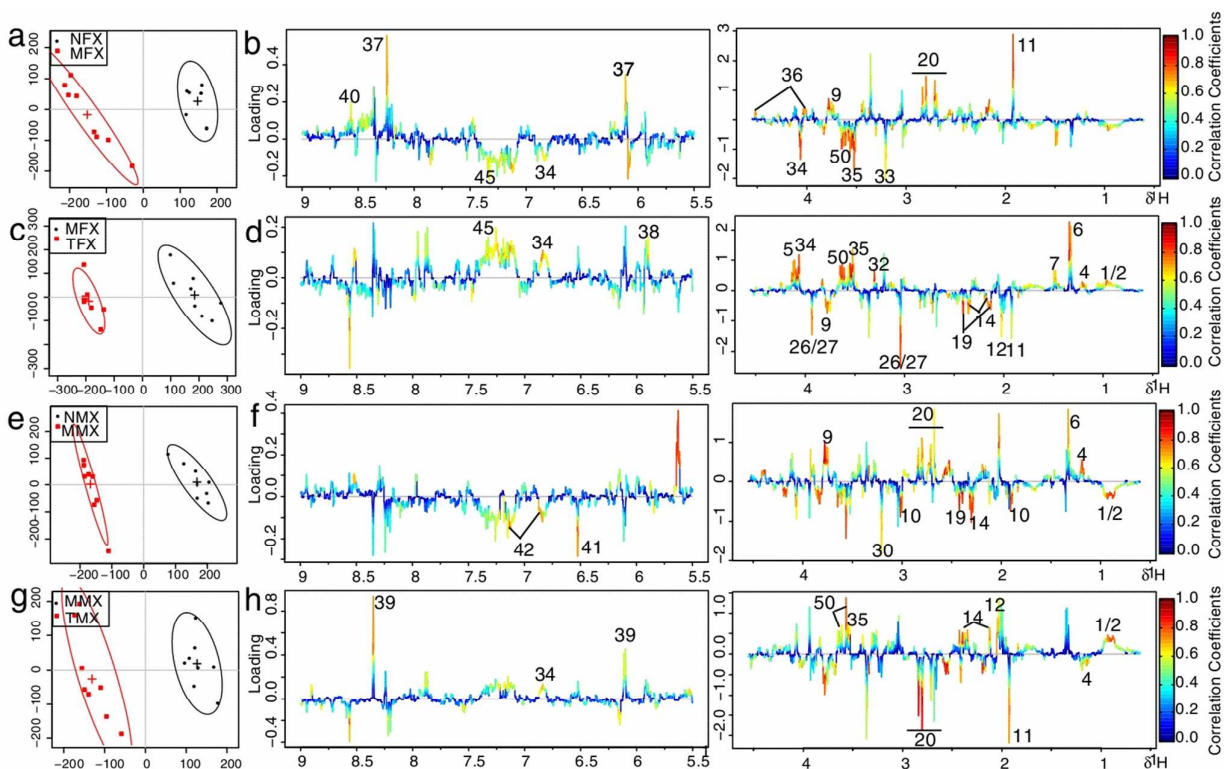
Fig. 9 OSC-PLS-DA analysis of cerebellum extracts ^{1}H NMR dataset of NF, MF, DF, NM, MM, and DM.. Scores plots (a, c, e and g) and the loading plot of OSC-PLS-DA (b, d, f and h) were analyzed after the removal of H_2O signals. Metabolite variation was visualized by the color-coded loading plots. Metabolites: 1, Ile; 2, Leu; 4, 3-HB; 5, Threonine; 6, Lac; 7, Ala; 9, Arg; 10, GABA; 11, AC; 12, NAA; 14, Glu; 19, Gln; 20, Asp; 26, Cr; 27, PCr; 30, OPC; 32, Tau; 33, Bet; 34, Myo; 35, Gly; 36, Asc; 37, Ino; 38, UDP; 39, Ade; 40, AMP; 41, Fum; 42, Tyr; 45, Phe.

3.9.2.2 Male rats

The same OSC-PLS-DA analyses were performed on cerebrum tissue and cerebellum tissue of male rats. In the scores plots (Fig. 8e and 9e), good separations were achieved between NM and MM ($R^2Y = 0.95$ and $Q^2Y = 0.88$ for cerebrum and $R^2Y = 0.94$ and $Q^2Y = 0.86$ for cerebellum, respectively) (Fig. 11c and g). The loading plots (Fig. 8f and 9f) and S-plots (Fig. 10 e and g) revealed that the MM group had increase of leucine, isoleucine, valine, 3-HB, lysine, acetoacetate, GABA, glutamate, glutamine, glycine, serine and AMP in cerebrum tissue; leucine, isoleucine, glutamate, glutamine, GABA, arginine, OPC, serine, hypoxanthine, creatinine, myo-inositol and glycine in cerebellum tissue; and decrease of acetate, GSH, acetone,

462   NAA, Cretine, PCr, betaine, malate and citrate in cerebrum tissue; NAA, tryptophan,

463   citrate, betaine and malate in cerebellum tissue.
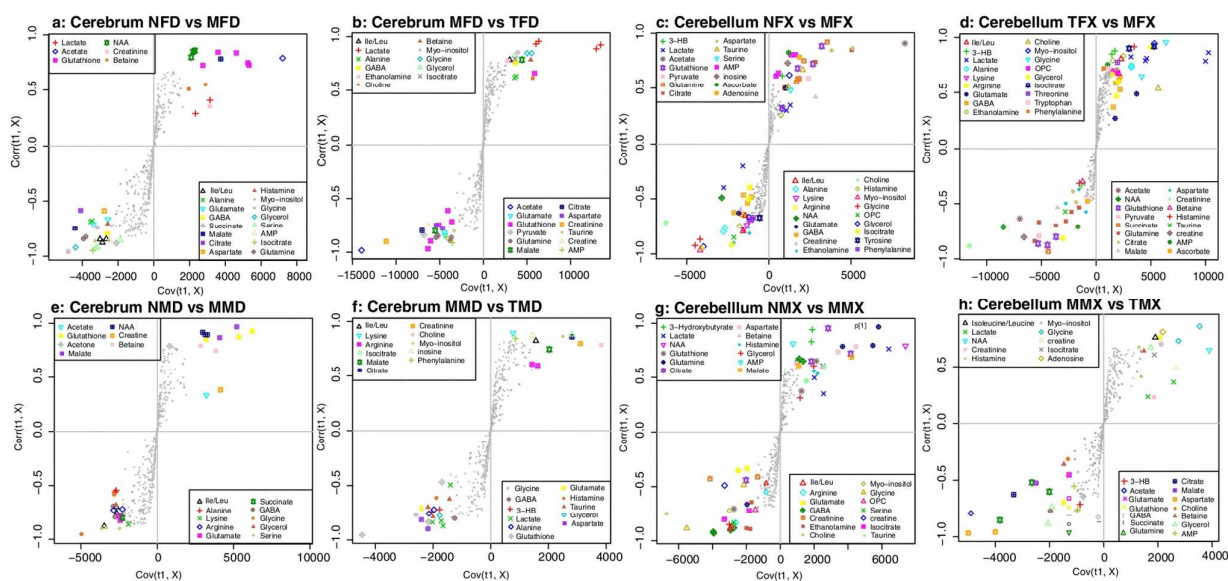
464

465   **Fig. 10** Color-coded S-plots for OSC-PLS-DA analysis of ^{1}H NMR data in cerebrum (a, b, e, f) and cerebellum (c,

466   d, g and h) for N, M and HLJDD-treated female rats (a, b, c and d)and male rats (e, f, g and h).
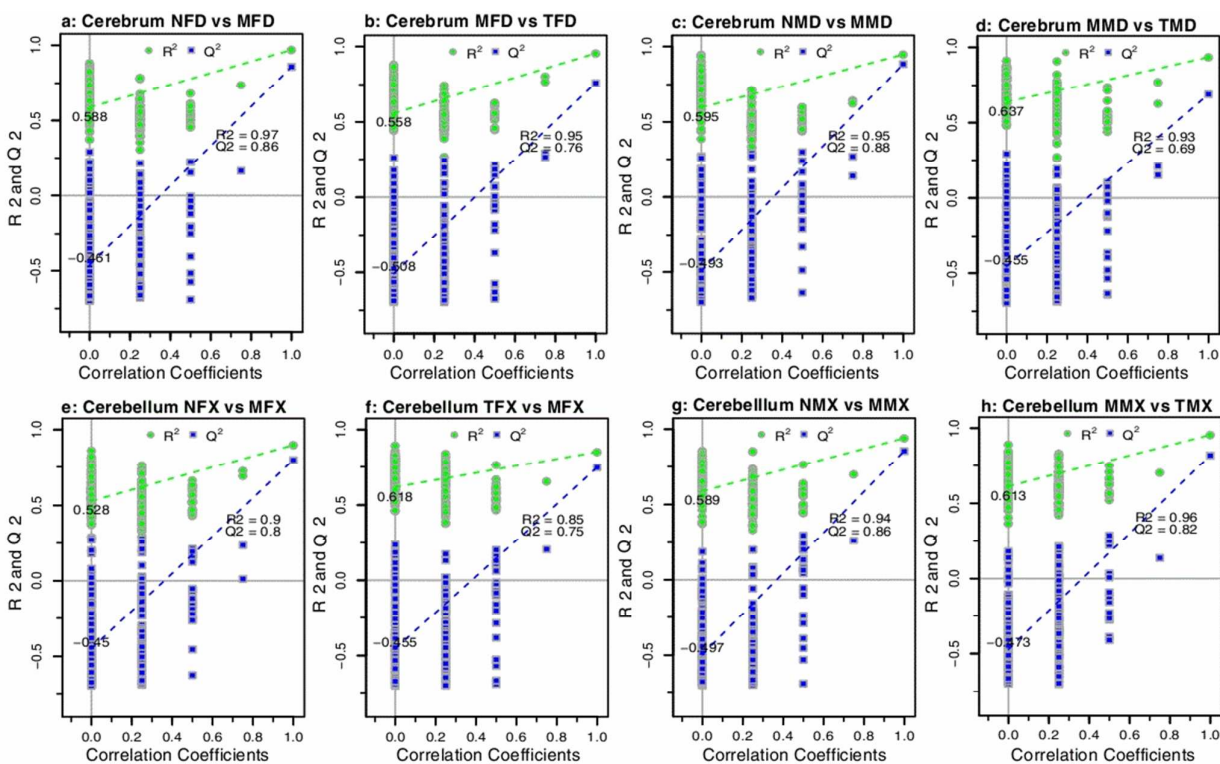
467

468   **Fig. 11** OPLS-DA scatter plot from cerebrum (a-d) and cerebellum (e-h) of the statistical validations obtained by

469   200 times permutation tests, with R^2 and Q^2 values in the vertical axis, the correlation coefficients (between the

470   permuted and true class) in the horizontal axis, and OLS line representing the regression of R^2 and Q^2 on the

471   correlation coefficients.

472   3.9.3 Gender specific metabolic changes in MCAO rats

473   ^{1}H NMR has revealed a panel of alterations that have taken place in serum,

474   cerebrum and cerebellum induced by MCAO. To further explore the gender-related

475   metabolic events, the changed metabolites in females were compared with male

476   groups by univariate analysis. The fold change values of metabolites in sham rats

477   relative to the MCAO groups and the associated p-values adjusted by

478   Benjamini-Hochberg were calculated and visualized by fold change plots (Fig. S1).

479   Color key indicates the metabolite expression value: red represents the highest and

480   blue represents the lowest. From the fold change plots, we could see that 20

481   compounds (LDL/VLDL, PUFA, 3-HB, acetate, acetoacetate, glucose, pyruvate,

482   citrate, malate, lactate, creatine, PCr, creatinine, choline, OPC, phenylalanine, tyrosine,

483   tryptophan and NAA) are of particular interest because they showed an explicit

484   difference between the two genders and can be considered candidate biomarkers for

485   gender characterization. Furthermore, they are naturally occurring metabolites that are

486   conserved in important metabolic pathways, such as oxidative stress, energy

487   metabolism, fat metabolism or amino acid metabolism.

488   3.9.4 Effect of HLJDD on the gender-related metabolic profiles of MCAO

489   The OSC-PLS-DA score plots (Fig. 7b, 8c and g, 9 c and g) showcased the ability of

490   HLJDD to protect against metabolic disturbance following the injury of

491   ischemia/reperfusion. To evaluate the metabolic consequences of female and male

492   MCAO rats treated with HLJDD and probe into the underlying treatment mechanisms

493   for HLJDD, the loadings plots (Fig 7d, 8d and h, 9d and h) and S-plots (Fig 7f, 10b, d,

494   f and h) were used to select significant metabolite changes due to HLJDD

495   administration in serum, cerebrum and cerebellum. The variations of identified

496   metabolites in different genders were visualized as color table (Table 1). The 20

497   gender-related potential biomarkers were selected to partly represent the disease status,

498   and they could be used to assess the efficacy of the treatmet in the two genders. The

499   significantly changed levels of metabolites in male MCAO rats, such as glucose,

500   pyruvate, citrate, malate, creatine, PCr, creatinine, LDL/VLDL, 3-HB, acetoacetate

501   and NAA, were reversed after HLJDD pretreatment. In addition, HLJDD could

502   reverse the levels of leucine, isoleucine, valine, choline and phosphocholine markedly

503   in female MCAO rats and slightly in MCAO male rats, suggesting a better protection

504   of HLJDD against CI/R injury in female rats.

505   **Table 1** Identified metabolites from different groups with fold change and P value.

|	Mebabolite	FC^{F}N_M	P^{F}N_M	FC^{F}N_T	P^{F}N_T	FC^{F}N_H	P^{F}N_	FC^{M}N_M	P^{M}N_M	FC^{M}N_T	P^{M}N_T	FC^{M}N_H	P^{M}N_H
Serum	Alanine	1.49		1.18		1.40		0.54	***	0.52	***	0.59	**
	OAG	1.14		2.12	***	1.67	***	1.13	*	1.41	**	1.09	
	Ile/Leu	1.11		1.37	***	1.26	***	1.19	***	1.25	**	1.03	
	Lactate	1.11		1.62		1.11		1.45	**	1.39	*	1.80	**
	NAG	1.08		1.66	***	1.23	**	1.33	***	1.49	**	1.02	
	creatinine	1.08		1.35	***	1.37	***	1.11	**	1.10		1.10	
	Glucose	1.07		1.02		1.13		0.79		0.86	*	0.94	
	PCr	1.07		1.03		1.10		0.85	*	0.93		0.94	
	creatine	1.05		1.63	***	1.58	***	0.85	*	1.13		0.82	
	PUFA	1.02		0.70	**	0.79	*	1.21	*	0.90		0.75	
	Citrate	1.02		1.15	**	1.35	***	0.85	*	0.92		0.99	
	pyruvate	1.02		1.18		1.56	***	0.56	***	0.70	**	0.86	
	LDL/VLDL	0.96		1.04		0.94		1.28	***	1.10		1.20	*
	Acetoacetate	0.77		0.48	***	0.54	***	0.62	**	1.27	*	0.80	
	3–HB	0.54		0.34	***	0.36	***	0.74	**	1.17	*	0.82	
Cerebrum	Phenylalanine	1.59	**	1.33		1.17		1.21		1.31		1.10	
	Tryptophan	1.54	**	1.25	*	0.96		1.24		1.16		1.23	
	Valine	1.50	*	1.21		1.17		1.13		1.31		0.91	
	Tyrosine	1.41	**	1.36	**	1.05		1.15		1.15		1.27	
	Ile/Leu	1.32	***	1.17	*	0.99		1.32	*	1.25		0.93	
	Citrate	1.26		1.51	***	0.96		0.80	**	0.84		1.02	
	Choline	1.24	*	1.05		0.97		1.20	**	1.23	*	1.09	
	Glycine	1.13	***	0.98		0.97		1.14	**	1.04		1.07	
	GABA	1.13	*	1.01		0.95		1.11	*	1.07		1.08	
	Glutamate	1.11	*	1.21	***	1.13	*	1.05	**	1.01		1.03	
	Aspartate	1.11		1.18	***	0.95		1.07	**	0.73		0.97	
	Malate	1.07		1.12	***	0.98	*	0.90	**	0.88		1.01	
	OPC	1.07		0.93	*	0.75	***	1.16	**	0.82		0.89	*
	NAA	1.08	*	0.60	**	1.39	**	0.57	***	0.48	***	1.06	
	Acetoacetate	1.18		0.96		0.94		1.14	**	1.05		1.06	*
	Taurine	1.06		1.16	**	1.16	*	1.07	**	1.11		0.96	
	Creatinine	1.02		1.10	**	1.08	*	1.10	*	1.01		1.06	
	Pyruvate	0.97		1.07		0.85	*	0.89	**	1.00		1.02	
	3–HB	0.96		0.90		0.99		1.27	*	0.92		0.78	
	Creatine	0.94	*	1.09		0.89	**	0.96		0.86		1.12	**
	Glutathione	0.88	**	0.96		1.09	*	0.90	**	0.96		0.98	
	Acetate	0.82	*	1.26	**	1.03		0.89	**	1.16	*	1.10	
Cerebellum	OPC	1.60	**	1.08		1.15	**	1.29	*	1.30	*	1.44	**
	Phenylalanine	1.37	*	0.99		1.22		1.15		1.08		1.15	
	Tryptophan	1.37	*	0.90		1.15		0.94		0.91		1.21	
	NAA	1.34	*	3.10	**	4.22	***	0.45	**	0.37	***	0.93	
	Citrate	1.32		6.74		21.20	***	0.12	**	0.98		1.03	
	Choline	1.30	*	1.11		1.01		1.35	*	1.36	*	1.07	
	Tyrosine	1.24	*	0.98		1.11		0.85		0.85		1.19	
	Glycine	1.14	***	1.00		1.01		1.12	**	0.99		1.08	**
	GABA	1.08		0.96		0.95		1.16	**	1.18	**	1.13	**
	Arginine	1.04		0.95		0.91		1.19	**	1.21	**	1.18	**
	Glutamate	1.03		1.05		1.08	*	1.15	*	1.09		1.09	
	Creatine	1.02		1.11	**	1.08		1.05		0.99		1.08	**
	Creatinine	1.00		1.18		1.11		1.07	**	1.07		1.12	**
	Taurine	0.95		0.99		0.96		0.88		0.88		0.92	
	Pyruvate	0.95		1.08		1.00		0.66	**	1.01		0.98	
	Malate	0.96		0.91		0.96		0.85	**	1.12		1.21	*
	Aspartate	1.01		0.87	**	0.89		1.31	*	1.10		1.03	
	Acetate	1.01		1.00		1.18		0.92	*	1.40		1.34	
	Acetoacetate	1.02		0.81		1.03		1.14	*	1.03		1.19	

−1.0   −0.5   0.0   0.5   1.0
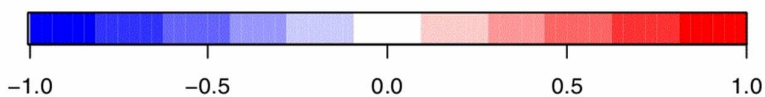
506

507   The FC and P means fold change and P value respectively (* P< 0.05, ** P< 0.01 and *** P< 0.001);

508   the superscript "F" and "M" means NC female and male respectively;

509   the N_M, N_T and N_H means N vs M, N vs D and N vs Y respectively.

510   Color coded according to $\log_2$(fold change) using the color bar labeled at the bottom.

511   3.10 Metabolite pathway analysis

512   Significant metabolites selected based on OSC-PLS-DA loading/S-plots and fold

513   change   plots   were   subjected   to   pathway   analysis   using   MetPA

514   (http://www.metaboanalyst.ca) to explore biologically meaningful metabolic patterns

515   and the most impacted pathways. Combining the results of powerful pathway

516   enrichment analysis with the topology analysis, MetPA estimated the disturbed

517   pathways in a more robust fashion than conventional approaches, making the

518   biological inference more reliable. A hypergeometric test using over-representation

519   analysis and pathway topology analysis of MetPA (Table S4), indicated that TCA cycle,

520   synthesis and degradation of ketone bodies, aminoacyl-tRNA biosynthesis, glycine,

521   serine and threonine metabolism, taurine and hypotaurine metabolism, alanine,

522   aspartate and glutamate metabolism, D-glutamine and D-glutamate metabolism, and

523   glutathione metabolism were disturbed in MCAO group rats (Fig. 12). Thus, based on

524   the above pathway analysis, a map of the MCAO-related metabolic pathways was

525   constructed (Fig. 13).

526
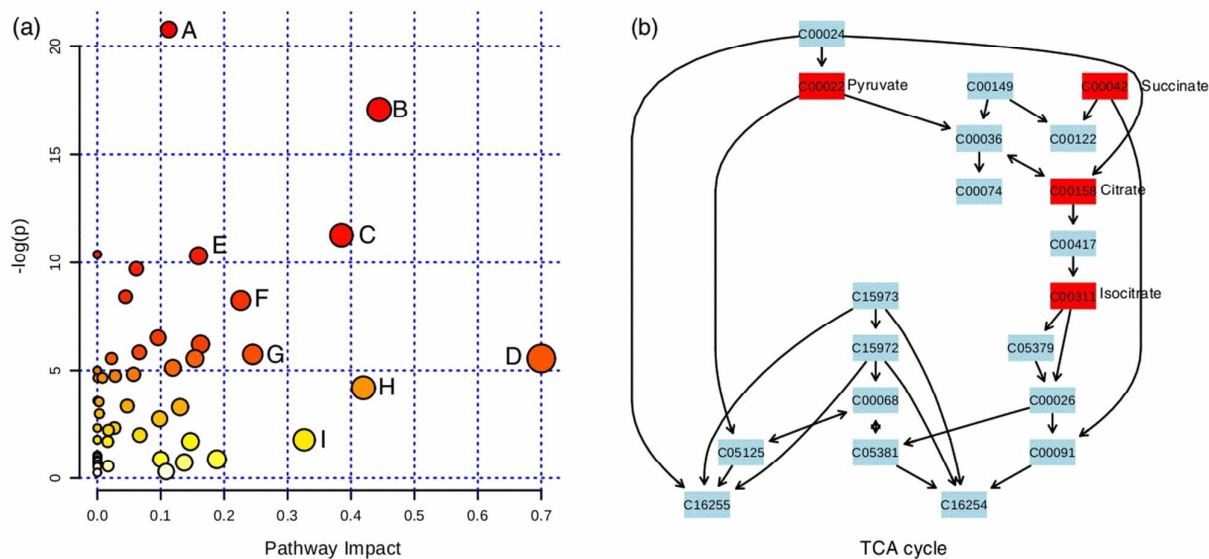
Fig. 12 Pathway topology analysis associate with MCAO was carried out by MetaboAnalyst in this study (a); and the pathway flowchart of impacted TCA cycle (b). The term "log P" is the transformation of original P value calculated from the enrichment analysis and the term "Impact" is the pathway impact value calculated from the pathway topology analysis. Bubble area is proportional to the impact of each pathway, with color denoting the significance from highest in red to lowest in white. Aminoacyl-tRNA biosynthesis (A); Glycine, serine and threonine metabolism (B); Taurine and hypotaurine metabolism (C); Synthesis and degradation of ketone bodies (D); Alanine, aspartate and glutamate metabolism (E); Citrate cycle (TCA cycle) (F); Glutathione metabolism (G); D-Glutamine and D-glutamate metabolism(I).
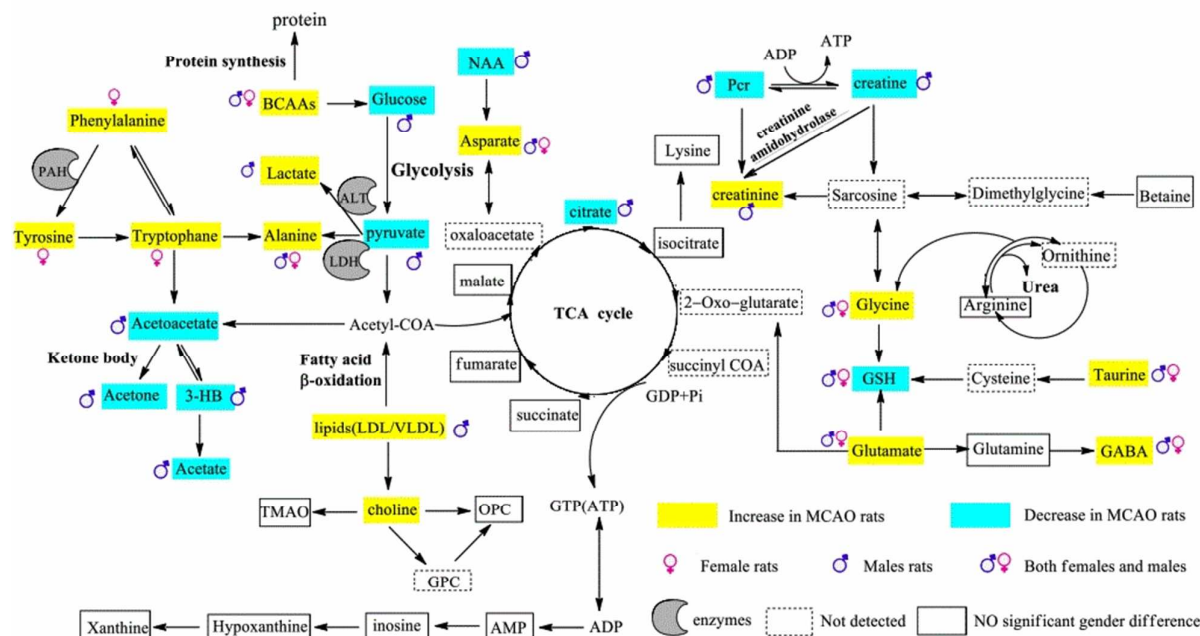
535

Fig. 13 Schematic diagram of the disturbed metabolic pathways detected by ^{1}H NMR analysis, showing the

537 interrelationship of the identified metabolites.

538

4. Discussion

540 In this study, complemented with serum and tissue biochemistry, histopathology and

541 immunohistochemistry, a ^{1}H NMR-based metabolomics approach was adopted to

542 investigate the gender specific metabolic events in ischemic stroke induced by MCAO

543 and the protective effect of HLJDD. Compared with sham rats, rats in MCAO groups

544 showed sluggish, poor ability of reflexes and did not fully stretch the left forepaw with

545 significantly increased neurological deficit scores at 24 h after reperfusion, revealing

546 severely impaired brain function due to cerebral ischemia-reperfusion (CI/R). HLJDD

547 could markedly improve the neurological function of ischemic stroke rats in both

548 females and males, consistent with the results of biochemical, tissue histopathological

549   and immunohistochemical inspections. Female rats were more resistant to stroke than

550   male rats, in consistent with several previous reports. One of the reasons might be the

551   beneficial effects of estrogen on cerebral circulation.[38] With vascular and

552   neuroprotective effects, estrogen could improve blood flow during and after an

553   ischemic insult.[39-45] OSC-PLS-DA analysis of NMR data from serum, cerebrum and

554   cerebellum revealed metabolic perturbations induced by MCAO in oxidative stress,

555   energy metabolism, fat metabolism and amino acid metabolism, and a series of

556   potential biomarkers for gender specific response to MCAO induced stroke.

557   4.1. Oxidative stress

558   Oxidative stress reflects an imbalance between the generation of reactive oxygen

559   species (ROS) and antioxidant defenses, which has been demonstrated to be a major

560   mechanism involved in CI/R injury.[46-48] Oxidative stress results in an accumulation of

561   ROS, and excessive ROS bring damage to DNA, cellular lipid and proteins, even

562   ultimately leading to cell death.[49] Several biochemical parameters were measured to

563   reflect the status of oxidative stress including NO, MDA, GSSH, SOD, GSH and

564   GSH-PX. ROS reacts readily with excessive endogenous NO to form neurotoxic

565   peroxynitrite, notorious in the process of neuronal damage triggered by CI/R.[50] MDA

566   is a lipid peroxidation product whose formation is accelerated by oxidative stress. The

567   endogenous defense system, primarily the antioxidant enzyme systems, e.g. SOD and

568   GSH-PX, and low-molecular weight ROS scavenger, such as GSH, could react with

569   free radicals directly[51] and attenuate the damage caused by ROS, and thereby mitigate

570   CI/R induced injury.[52, 53] The significantly elevated levels of NO, MDA and GSSH,

571 and decreased levels of GSH, GSH-PX and SOD demonstrated ROS generation and

572 oxidative stress occurring in the MCAO rats. HLJDD pretreatment could ameliorate

573 these abnormal parameters in both females and males as revealed by decreased

574 contents of NO, MDA and GSSG, and increased level of GSH, GSH-PX and SOD, as

575 compared with the MCAO rats.

576 Mitochondria are the primary sites for ROS generation, which make them especially

577 vulnerable to oxidative damage. The significant inhibition of the activities of

578 Na^+/K^+-ATPase and Ca^{2+}-ATPase in the MCAO groups indicated a severe dysfunction

579 in the mitochondrial energy metabolism brought by CI/R. CI/R could affect

580 mitochondrial membrane permeability, resulting in inner membrane permeabilization,

581 outer membrane rupture, and cell apoptosis,[54] which was demonstrated by the notably

582 elevated activities of rccaspase-3 (one of the key initiative of the apoptotic signaling

583 pathways), GFAP (the major protein constituent of glial intermediate filaments in

584 differentiated fibrous and protoplasmic astrocytes of the central nervous system), p65

585 (the subunit of the transcription factor NF-κB) and VEGF (a key regulator of

586 physiological and pathological angiogenesis) in MCAO rats according to

587 immunohistochemical inspection. HLJDD could markedly increase the activities of

588 Na^+/K^+-ATPase and Ca^{2+}-ATPase, and decrease those of caspase-3, GFAP, p65 and

589 VEGF in MCAO rats.

590 Compared with the sham rats, significantly increased levels of glutamate, glycine,

591 choline, phosphocholine (OPC), NAG, OAG and branched chain amino acids (BCAAs,

592 leucine, isoleucine and valine) were observed in both female and male MCAO rats,

593   also indicative of a status of oxidative stress. The increase of glutamate and glycine

594   might be a consequence of an inhibited GSH synthesis, and the increased levels of

595   choline and OPC demonstrated membrane damage, which possibly leading to

596   enhanced membrane permeability and altered membrane structure, indicated by the

597   increased levels of NAG and OAG since that they were synthesized in membranes of

598   endoplasmic reticulum and golgi apparatus. In addition, the elevated levels of BCAAs

599   in serum and cerebrum suggested protein degradation by ROS. HLJDD decreased the

600   elevated brain level of glutamate, glycine, choline, OPC and BCAAs markedly in

601   female MCAO rats and slightly in male MCAO rats (Table 1), showcasing a better

602   protection of HLJDD against ischemic stroke-induced oxidative injury in female rats

603   than in male rats.

604   4.2 Energy metabolism

605   Compared with the normal rats, levels of glucose, pyruvate, citrate and malate were

606   significantly decreased; the level of lactate was obviously increased in male MCAO

607   rats, which was not observed in female MCAO rats. The supply of glucose and oxygen

608   in brain was blocked in cerebral ischemia due to insufficient blood supply. Pyruvate is

609   generated in the first step of glucose metabolism, generating a small amount of ATP,

610   which can be used to produce acetyl-CoA by pyruvate dehydrogenase complex.

611   Acetyl-CoA enters into TCA cycle and plays a key role in glucose aerobic oxidation

612   and energy production. As the important intermediates of the TCA cycle, the

613   decreased levels of citrate and malate in serum, cerebrum and cerebellum of the male

614   MCAO rats might suggest an marked inhibition of the TCA cycle.[55] TCA cycle is the

615   most efficient and major source of energy supply, the inhibition of which brought

616   about energy deficiency, so other means, such as glycolysis, come to rescue. By

617   glycolysis, pyruvate is converted to lactate by lactate dehydrogenase (LDH), resulting

618   in increased levels of lactate.[53] The marked decrease of glucose and pyruvate, and

619   increase of lactate in serum of male MCAO rats demonstrated an enhanced anaerobic

620   glycolysis.

621   Marked decrease of creatine and phosphocreatine (PCr), and increase of creatinine

622   in serum were observed in the male MCAO rats. The creatine-PCr system is crucial

623   for the balance of energy supply.[56-58] When the energy demand outstrips its supply, the

624   high-energy phosphate bond in PCr could be transferred to adenosine diphosphate

625   (ADP) under the catalysis of creatine kinase (CK) to form ATP for energy demand,

626   liberating creatine, which subsequently degraded to creatinine. The decrease of PCr

627   and creatine, and the increase of creatinine thus suggested an enhanced utilization of

628   PCr to produce extra energy to meet the unmet energy demand.

629   All these results indicated that energy metabolism was severely damaged in male

630   MCAO rats but not so in female MCAO rats, which might be an important reason for

631   the resistance of female rats to ischemic stroke. HLJDD greatly improved the damaged

632   energy metabolism in male MCAO rats, as evidenced by its ability to apparently

633   increase the levels of glucose, pyruvate and citrate, and decrease the levels of lactate

634   in male MCAO rats. With the improvement of energy supply, other means of energy

635   production are not at all necessary, exemplified by the elevated levels of creatine and

636   PCr, and reduced level of creatinine in male MCAO rats.

4.3 Fat metabolism

Significantly increased levels of lipids (LDL/VLDL) and PUFA were observed only in serum of male MCAO rats, showing great gender specific difference. The increase of free fatty acids (LDL/VLDL and PUFA) indicated an inhibition of fatty acid β-oxidation in male MCAO rats, resulting in an insufficient supply of acetyl-CoA to participate in the TCA cycle, thus necessitating the conversion of ketone bodies to acetyl-CoA to replenish acetyl-CoA consumed in the TCA cycle as the energy source. Ketone bodies, such as 3-HB and acetoacetate, could also serve as fuel in the case of starving of brains. They could be transferred from serum to brain to replenish insufficient energy supply,[53] which was supported by their observed decrease and increase, in serum and brain (Table 1), respectively. Such an inhibition of fatty acids β-oxidation was also indicated by the observed decrease of acetate.

Compared with the male MCAO rats, LDL/VLDL was decreased and acetoacetate and 3-HB were increased in serum after treatment with HLJDD, which indicated an enhanced fatty acid β-oxidation. As a result, the level of acetate was increased in the cerebrum of male HLJDD-treated MCAO rats.

4.4 Amino acid metabolism

In our study, the female and male MCAO groups showed significant increase in both excitatory amino acids (glutamate, asparate) and inhibitory AAs (GABA, glycine) levels in cerebrum, elucidating cerebrum damage. Since the discovery of ischemia-evoked releases of glutamate and asparate in the rat hippocampus,[59] evidence has accumulated during the past two decades showing that the excessive release of

659 excitatory amino acids (EAA) such as glutamate or asparate is the pathological

660 mechanism behind ischemic cerebrum damage.[60] Inhibitory AAs, such as GABA,

661 taurine and glycine, have also been reported to be released during cerebral ischemia as

662 a protection to alleviate the severity of ischemic injury and to counteract the toxicity

663 of excitatory AAs.[60] After HLJDD treatment, glutamate, asparate, GABA and glycine

664 were restored to the normal levels, indicating that HLJDD could not only restore the

665 increased levels of excitatory neurotransmitters in MCAO, but also is good in the

666 restoration of the level of inhibitory neurotransmitters in MCAO. HLJDD offers

667 protection against cerebrum damage in both excitatory and inhibitory

668 neurotransmitters with no gender difference.

669   We also found that the aromatic amino acids (AAAs), such as phenylalanine

670 (FC=1.59, p<0.01), tyrosine (FC=1.41, p<0.01) and tryptophan (FC=1.54, p<0.01)

671 were higher in the MCAO females than they were in the normal females, whereas no

672 significant difference of them (p>0.05) were observed between the MCAO and normal

673 males (Table 1). Phenylalanine significantly and reversibly inhibits excitatory

674 glutamatergic synaptic transmission (GST) via a unique set of presynaptic and

675 postsynaptic mechanisms, and may represent a new therapeutic approach to mitigate

676 the consequences of ischemic stroke.[61] Tyrosine is referred to a semi-essential or

677 conditionally indispensable amino acid because it can only be synthesized by the

678 hydroxylation of phenylalanine catalyzed by phenylalanine hydroxylase (PAH).

679 Tryptophan is metabolized via several pathways, one of which is the kynurenine

680 pathway for tryptophan oxidation resulting in kynurenic acid, which can afford

681   neuroprotection against brain damage arising from ischemia, hypoxia or traumatic

682   brain injury.[62] The increase of AAAs in MCAO female rats were thus beneficial for

683   their recovery in stroke, and might be also a reason for their resistance to stroke.

684   Interestingly, we observed significantly decreased levels of N-acetylaspartic acid

685   (NAA) in cerebrum and cerebellum of male stroke rats, whereas, the level of NAA is

686   increased slightly in female stroke rats. NAA, the second most concentrated molecule

687   in the cerebrum after glutamate, is thought to be an amino acid that is specific to

688   neurons. Previous studies have furnished strong evidence to support the view that

689   NAA is an in vivo maker of neuronal density and its reduction is related to neuronal

690   damage and loss in many cerebral disorders.[63-68] HLJDD treatment cannot reverse the

691   changes of NAA occurred in MCAO rats.

692   In summary, the oxidative stress, energy metabolism, fat metabolism and amino

693   acid metabolism severely perturbed in male MCAO rats, while only oxidative stress

694   and amino acid metabolism were perturbed in female MCAO rats, indicating that

695   ischemic stroke tended to be more severe in male rats, and female rats were more

696   resistant to stroke than male rats. After the HLJDD treatment, these imbalanced

697   metabolites in TCA cycle, free fatty acids β-oxidation and amino acid metabolism in

698   male MCAO rats gravitated towards normal or negative control group, demonstrating

699   the treatment effects of HLJDD. Moreover, HLJDD also modulate ischemic stroke in a

700   gender dependent manner. Females appeared to gain a relatively greater benefit from

701   HLJDD therapy than males according to the analysis of metabolomics profiling.

702

5. Conclusions

In this study, an integrated ^{1}H NMR metabolomics approach was successfully applied to investigate gender specific metabolic pathways perturbed by MCAO and explore the gender difference in HLJDD treatment on focal cerebral ischemia. Only slight differences between genders were observed in conventional clinical chemistry, histopathological and immunohistochemical evaluations. However, ^{1}H NMR-based metabolomics analysis successfully revealed a panel of endogenous metabolites that are relevant to gender different responses to stroke, manifesting the sensitivity and advantage of metabolomics approach than traditional means. The results obtained confirmed the existence of gender difference in ischemic stroke and more resistance of female rats to stroke than male rats, and demonstrated that the effects of HLJDD on stroke were also gender-dependent. This study built a substantial basis for further systematic study on the underlying mechanisms involved in these gender differences in ischemic stroke. These findings also highlight the need to take gender differences into account in the treatment of stroke and the development of its therapy strategies.

Acknowledgments

725 **References**

726   1.   S. E. Lakhan, A. Kirchgessner and M. Hofer, *J Transl Med*, 2009, **7**, 97.

727   2.   Q. Shi, P. Zhang, J. Zhang, X. Chen, H. Lu, Y. Tian, T. Parker and Y. Liu, *Neuroscience letters*, 2009, **465**, 220-225.

728   3.   F. Palm, C. Urbanek, S. Rose, F. Buggle, B. Bode, M. G. Hennerici, K. Schmieder, G. Inselmann, R. Reiter and R.
729   Fleischer, *Stroke*, 2010, **41**, 1865-1870.

730   4.   C. Sudlow and C. Warlow, *Stroke*, 1997, **28**, 491-499.

731   5.   S. Renolleau, S. Fau and C. Charriault-Marlangue, *The Neuroscientist*, 2007.

732   6.   J. G. Canto, M. G. Shlipak, W. J. Rogers, J. A. Malmgren, P. D. Frederick, C. T. Lambrew, J. P. Ornato, H. V. Barron
733   and C. I. Kiefe, *Jama*, 2000, **283**, 3223-3229.

734   7.   A. W. Jones, *Addiction*, 2007, **102**, 1085-1091.

735   8.   A. W. Jones, A. Holmgren and F. C. Kugelberg, *Addiction*, 2008, **103**, 452-461.

736   9.   M. Djurendic-Brenesel, M. Mimica-Dukic, V. Pilija and M. Tasic, *Forensic science international*, 2010, **194**, 28-33.

737   10.   A. Hines, W. H. Yeung, J. Craft, M. Brown, J. Kennedy, J. Bignell, G. D. Stentiford and M. R. Viant, *Analytical*
738   *biochemistry*, 2007, **369**, 175-186.

739   11.   M. P. Hodson, G. J. Dear, A. D. Roberts, C. L. Haylock, R. J. Ball, R. S. Plumb, C. L. Stumpf, J. L. Griffin and J. N.
740   Haselden, *Analytical biochemistry*, 2007, **362**, 182-192.

741   12.   S. Kochhar, D. M. Jacobs, Z. Ramadan, F. Berruex, A. Fuerholz and L. B. Fay, *Analytical biochemistry*, 2006, **352**,
742   274-281.

743   13.   R. S. Plumb, J. H. Granger, C. L. Stumpf, K. A. Johnson, B. W. Smith, S. Gaulitz, I. D. Wilson and J. Castro-Perez,
744   *Analyst*, 2005, **130**, 844-849.

745   14.   R. Plumb, J. Granger, C. Stumpf, I. D. Wilson, J. A. Evans and E. M. Lenz, *Analyst*, 2003, **128**, 819-823.

746   15.   C. M. Slupsky, K. N. Rankin, J. Wagner, H. Fu, D. Chang, A. M. Weljie, E. J. Saude, B. Lix, D. J. Adamko and S. Shah,
747   *Analytical chemistry*, 2007, **79**, 6995-7004.

748   16.   N. G. Psihogios, I. F. Gazi, M. S. Elisaf, K. I. Seferiadis and E. T. Bairaktari, *NMR in Biomedicine*, 2008, **21**,
749   195-207.

750   17.   N. J. Serkova, T. J. Standiford and K. A. Stringer, *American journal of respiratory and critical care medicine*, 2011,
751   **184**, 647-655.

752   18.   E. Holmes, *xenobiotica*, 1999, **29**, 1181-1189.

753   19.   Z. Pan and D. Raftery, *Analytical and bioanalytical chemistry*, 2007, **387**, 525-527.

754   20.   M. Coen, E. Holmes, J. C. Lindon and J. K. Nicholson, *Chemical research in toxicology*, 2008, **21**, 9-27.

755   21.   S. Zhang, G. N. Gowda, V. Asiago, N. Shanaiah, C. Barbas and D. Raftery, *Analytical biochemistry*, 2008, **383**,
756   76-84.

757   22.   X. Zhang, H. Liu, J. Wu, X. Zhang, M. Liu and Y. Wang, *Neurochemistry international*, 2009, **54**, 481-487.

758   23.   H. Nagasawa and K. Kogure, *Recent Advances in the Pharmacology of Kampo (Japanese Herbal) Medications.*
759   *Excerpta Medica, Tokyo*, 1988, 223-226.

760   24.   T. Itoh, *Kampo Newest Therapy*, 2001, **10**, 243-246.

761   25.   K. Kawashima, N. Haruo and K. Kogure, *Pharma Medica*, 1988, **6**, 33-37.

762   26.   Y. Kondo, F. Kondo, M. Asanuma, K.-i. Tanaka and N. Ogawa, *Neurochem Res*, 2000, **25**, 205-209.

763   27.   Y. S. Hwang, C. Y. Shin, Y. Huh and J. H. Ryu, *Life sciences*, 2002, **71**, 2105-2117.

764   28.   J. Xu, Y. Murakami, K. Matsumoto, M. Tohda, H. Watanabe, S. Zhang, Q. Yu and J. Shen, *Journal of*
765   *ethnopharmacology*, 2000, **73**, 405-413.

766   29.   J. Lu, J.-S. Wang and L.-Y. Kong, *Journal of ethnopharmacology*, 2011, **134**, 911-918.

767   30.   D. Wei, S. Liao, J. Wang, M. Yang and L. Kong, *RSC Advances*, 2015, **5**, 66200-66211.

768   31.   P.-R. Wang, J.-S. Wang, M.-H. Yang and L.-Y. Kong, *Journal of pharmaceutical and biomedical analysis*, 2014, **88**,
769   106-116.
770   32.   P.-R. Wang, J.-S. Wang, C. Zhang, X.-F. Song, N. Tian and L.-Y. Kong, *Journal of ethnopharmacology*, 2013, **149**,
771   270-280.
772   33.   E. Z. Longa, P. R. Weinstein, S. Carlson and R. Cummins, *stroke*, 1989, **20**, 84-91.
773   34.   H. Nagasawa and K. Kogure, *Stroke*, 1989, **20**, 1037-1043.
774   35.   J. Lindon, R. Farrant, P. Sanderson, P. Doyle, S. Gough, M. Spraul, M. Hofmann and J. Nicholson, *Magnetic*
775   *resonance in chemistry*, 1995, **33**, 857-863.
776   36.   O. Cloarec, M. E. Dumas, J. Trygg, A. Craig, R. H. Barton, J. C. Lindon, J. K. Nicholson and E. Holmes, *Analytical*
777   *Chemistry*, 2005, **77**, 517-526.
778   37.   J. M. Fonville, S. E. Richards, R. H. Barton, C. L. Boulange, T. Ebbels, J. K. Nicholson, E. Holmes and M. E. Dumas,
779   *Journal of Chemometrics*, 2010, **24**, 636-649.
780   38.   D. N. Krause, S. P. Duckles and D. A. Pelligrino, *Journal of Applied Physiology*, 2006, **101**, 1252-1261.
781   39.   D. A. Pelligrino, R. Santizo, V. L. Baughman and Q. Wang, *Neuroreport*, 1998, **9**, 3285-3291.
782   40.   L. D. McCullough, N. J. Alkayed, R. J. Traystman, M. J. Williams and P. D. Hurn, *Stroke*, 2001, **32**, 796-802.
783   41.   P. D. Hum, M. T. Littleton-Kearney, J. R. Kirsch, A. Dharmarajan and R. J. Traystman, *Journal of cerebral blood*
784   *flow and metabolism : official journal of the International Society of Cerebral Blood Flow and Metabolism*, 1995,
785   **15**, 666-672.
786   42.   T. Hawk, Y. Zhang, G. Rajakumar, A. L. Day and J. W. Simpkins, *Brain research*, 1998, **796**, 296-298.
787   43.   H. V. Carswell, N. H. Anderson, J. J. Morton, J. McCulloch, A. F. Dominiczak and I. M. Macrae, *Journal of Cerebral*
788   *Blood Flow & Metabolism*, 2000, **20**, 931-936.
789   44.   S.-H. Yang, J. Shi, A. L. Day and J. W. Simpkins, *Stroke*, 2000, **31**, 745-750.
790   45.   Y. Watanabe, M. Littleton-Kearney, R. Traystman and P. Hurn, *American Journal of Physiology-Heart and*
791   *Circulatory Physiology*, 2001, **281**, H155-H160.
792   46.   S. Cuzzocrea, D. P. Riley, A. P. Caputi and D. Salvemini, *Pharmacological reviews*, 2001, **53**, 135-159.
793   47.   M. C. Mendoza, E. E. Er and J. Blenis, *Trends in biochemical sciences*, 2011, **36**, 320-328.
794   48.   B. K. Siesjö, *Journal of neurosurgery*, 1992, **77**, 169-184.
795   49.   Y.-Q. Zheng, J.-X. Liu, J.-N. Wang and L. Xu, *Brain research*, 2007, **1138**, 86-94.
796   50.   X. Liu, H. Chen, B. Zhan, B. Xing, J. Zhou, H. Zhu and Z. Chen, *Biochemical and biophysical research*
797   *communications*, 2007, **359**, 628-634.
798   51.   C. Lu, Y. Wang, Z. Sheng, G. Liu, Z. Fu, J. Zhao, J. Zhao, X. Yan, B. Zhu and S. Peng, *Toxicology and applied*
799   *pharmacology*, 2010, **248**, 178-184.
800   52.   Y. Li, B. Jiang, T. Zhang, W. Mu and J. Liu, *Food chemistry*, 2008, **106**, 444-450.
801   53.   X. Chao, J. Zhou, T. Chen, W. Liu, W. Dong, Y. Qu, X. Jiang, X. Ji, H. Zhen and Z. Fei, *Brain research*, 2010, **1363**,
802   206-211.
803   54.   P. S. Brookes, Y. Yoon, J. L. Robotham, M. Anders and S.-S. Sheu, *American Journal of Physiology-Cell Physiology*,
804   2004, **287**, C817-C833.
805   55.   M. I. Shariff, A. I. Gomaa, I. J. Cox, M. Patel, H. R. Williams, M. M. Crossey, A. V. Thillainayagam, H. C. Thomas, I.
806   Waked and S. A. Khan, *Journal of proteome research*, 2011, **10**, 1828-1836.
807   56.   C. Ma, K. Bi, M. Zhang, D. Su, X. Fan, W. Ji, C. Wang and X. Chen, *Journal of pharmaceutical and biomedical*
808   *analysis*, 2010, **53**, 559-566.
809   57.   C. Ma, K. Bi, M. Zhang, D. Su, X. Fan, W. Ji, C. Wang and X. Chen, *Journal of ethnopharmacology*, 2010, **130**,
810   134-142.
811   58.   M. Wyss and R. Kaddurah-Daouk, *Physiological reviews*, 2000, **80**, 1107-1213.

812 59. P. Saransaari and S. S. Oja, *Brain research*, 1998, **807**, 118-124.

813 60. X. Bie, Y. Chen, J. Han, H. Dai, H. Wan and T. Zhao, *Asia Pac J Clin Nutr*, 2007, **16**, 305-308.

814 61. T. Kagiyama, A. V. Glushakov, C. Sumners, B. Roose, D. M. Dennis, M. I. Phillips, M. S. Ozcan, C. N. Seubert and A.
815   E. Martynyuk, *Stroke*, 2004, **35**, 1192-1196.

816 62. A.-M. Myint, Y. K. Kim, R. Verkerk, S. Scharpé, H. Steinbusch and B. Leonard, *Journal of affective disorders*, 2007,
817   **98**, 143-151.

818 63. R. Brenner, P. Munro, S. C. Williams, J. D. Bell, G. Barker, C. Hawkins, D. Landon and W. McDonald, *Magnetic*
819   *resonance in medicine*, 1993, **29**, 737-745.

820 64. T. N. Sager, H. Laursen, A. Fink-Jensen, S. Topp, A. Stensgaard, M. Hedehus, S. Rosenbaum, J. S. Valsborg and A.
821   J. Hansen, *Journal of Cerebral Blood Flow & Metabolism*, 1999, **19**, 164-172.

822 65. T. N. Sager, H. Laursen and A. J. Hansen, *Journal of Cerebral Blood Flow & Metabolism*, 1995, **15**, 639-646.

823 66. L. Harms, H. Meierkord, G. Timm, L. Pfeiffer and A. Ludolph, *Journal of Neurology, Neurosurgery & Psychiatry*,
824   1997, **62**, 27-30.

825 67. T. Ebisu, W. D. Rooney, S. H. Graham, M. W. Weiner and A. A. Maudsley, *Journal of Cerebral Blood Flow &*
826   *Metabolism*, 1994, **14**, 373-382.

827 68. C. Davie, G. Barker, A. Thompson, P. Tofts, W. McDonald and D. Miller, *Journal of Neurology, Neurosurgery &*
828   *Psychiatry*, 1997, **63**, 736-742.

829